TÜRKİYE CUMHURİYETİ
ADANA ALPARSLAN TÜRKEŞ SCIENCE AND TECHNOLOGY UNIVERSITY

GRADUATE SCHOOL

BIOENGINEERING DEPARTMENT

PREPARATION OF MOLECULARLY IMPRINTED NANOPARTICLE-BASED SURFACE PLASMON RESONANCE (SPR) SENSORS FOR ANGIOTENSIN-II DETECTION FROM HUMAN SERUM

KARDELEN CEMEK ŞAHİN

Ph.D.

ADANA 2025

TÜRKİYE CUMHURİYETİ
ADANA ALPARSLAN TÜRKEŞ SCIENCE AND TECHNOLOGY UNIVERSITY

GRADUATE SCHOOL

BIOENGINEERING DEPARTMENT

PREPARATION OF MOLECULARLY IMPRINTED NANOPARTICLE-BASED SURFACE PLASMON RESONANCE (SPR) SENSORS FOR ANGIOTENSIN-II DETECTION FROM HUMAN SERUM

KARDELEN CEMEK ŞAHİN

Ph.D.

SUPERVISOR

PROF. GÖZDE BAYDEMİR PEŞİNT

ADANA, 2025

DECLARATION OF CONFORMITY

In this thesis study, which was prepared following the thesis writing rules of Adana Alparslan Türkeş Science and Technology University Institute of Graduate School, I declare that I provide all the information, documents, evaluations and results in accordance with scientific ethics and moral codes without resorting to any means or assistance that would be contrary to scientific ethics and traditions. I also declare that I refer to all of the articles I used in this study with appropriate references and accept all moral and legal consequences if a situation is found contrary to my statement regarding my work.

09/07/2025

[Signature]

Kardelen CEMEK ŞAHİN

ÖZET

İNSAN SERUMUNDAN ANJİOTENSİN-II TESPİTİ İÇİN MOLEKÜLER BASKILANMIŞ NANOPARTİKÜL TEMELLİ YÜZEY PLAZMON REZONANS (SPR) SENSÖRLERİNİN HAZIRLANMASI

Kardelen CEMEK ŞAHİN

Doktora, Biyomühendislik Anabilim Dalı

Danışman: Prof. Dr. Gözde BAYDEMİR PEŞİNT

Temmuz 2025, 88 sayfa

Anjiyotensin II (AgII), renin-anjiyotensin-aldosteron (RAAS) sisteminin işleyişinde görev alan kısa zincirli bir peptittir. Vücutta gerçekleşen birçok fizyolojik sürecin düzenlenmesinde aktif rol alır. Güçlü bir vazokonstriktör olarak işlev görür. Ayrıca sıvı-elektrolit dengesinin korunmasına da katkı sağlar. AgII'nin önemi yalnızca fizyolojik düzenleyici görevleriyle sınırlı değildir; aynı zamanda çeşitli kardiyovasküler ve metabolik hastalıklarda bir biyobelirteç (biomarker) olarak da değerlendirilir. Hipertansiyon, kalp yetmezliği ve kronik böbrek hastalığı gibi klinik durumlarda, plazma veya idrarda artmış AgII düzeylerinin gözlenmesi, bu hastalıkların altta yatan fizyolojik süreçlerine dair önemli ipuçları sunar. Bu bağlamda, AgII düzeylerinin ölçülmesi, söz konusu hastalıkların erken evrelerinde tanı koyma ve hastalık seyrini izleme açısından değerli bilgiler sağlamaktadır. Bu tez çalışmasında, insan serumundan AgII'yi tespit etmek için moleküler baskılanmış nanopartikül tabanlı yüzey plazmon rezonans (SPR) sensörlerinin geliştirilmesi amaçlanmıştır. Bu amaçla, moleküler baskılama yöntemi kullanılarak AgII-baskılanmış (AgII-MIP) ve baskılanmamış (NIP) nanopartiküller sentezlenmiştir. Sentezlenen nanopartiküller Zeta-boyut ölçümü, Geçirgen Elektron Mikroskobu (TEM), Taramalı Elektron Mikroskobu (SEM) ve FTIR Spektroskopisi teknikleri ile kapsamlı bir analizden geçirilmiştir. Zeta-boyut ölçümleri neticesinde, AgII-MIP ve NIP nanopartiküllerinin partikül boyutları sırasıyla 46.51 nm ve 48.97 nm olarak bulunmuştur. Nanopartiküller daha sonra SPR çipinin yüzeyini kaplamak için kullanılmıştır.

Böylelikle AgII-MIP nanopartikül kaplı SPR çip (AgII-MICspr) ve NIP nanopartikül kaplı SPR çip (NICspr) başarılı bir şekilde elde edilmiştir. Çiplerin Temas Açısı ve Atomik Kuvvet Mikroskobu ile karakterizasyon çalışmaları gerçekleştirilmiştir. Çeşitli konsantrasyonlarda AgII çözeltileri (3-100 pg/mL) hazırlanmış ve bu çözeltiler AgII-MICspr çipi ile etkileştirilmiştir. AgII-MICspr çipi, çok düşük AgII konsantrasyonu (3 pg/mL) için bile hassas tespit yeteneği göstermiştir. Ayrıca AgII-MICspr ve NICspr çipleri kullanılarak seçicilik çalışmaları da yapılmıştır. Burada, Anjiyotensin I (AgI) ve Vazopressin (Vp) yarışmacı olarak kullanılmıştır. AgII-MICspr çipinin AgII'ye karşı seçiciliğinin AgI ve Vp moleküllerine kıyasla sırasıyla 4.75 ve 5.43 kat daha yüksek olduğu belirlenmiştir. AgII-MICspr çipi kullanılarak tekrar kullanılabilirlik çalışmaları yapılmış ve 10 tekrar sonucunda dahi çipin bağlanma bölgelerindeki işlevselliğini koruduğu gözlenmiştir. İnsan serumundan AgII tespit çalışmaları yapılmıştır. Çip bu kompleks ortamdan çok düşük konsantrasyondaki AgII'yi seçici olarak tespit edebilmiştir.

Anahtar Kelimeler: Anjiyotensin II, Moleküler baskılama tekniği, SPR sensör, İnsan serumu.

ABSTRACT

PREPARATION OF MOLECULARLY IMPRINTED NANOPARTICLE-BASED SURFACE PLASMON RESONANCE (SPR) SENSORS FOR ANGIOTENSIN-II DETECTION FROM HUMAN SERUM

Kardelen CEMEK ŞAHİN

Ph.D., Department of Bioengineering
Supervisor: Prof. Gözde BAYDEMİR PEŞİNT

July 2025, 88 pages

Angiotensin II (AgII) is a short-chain peptide involved in the functioning of the renin-angiotensin-aldosterone (RAAS) system. It is actively involved in controlling many physiological activities within the human body. It acts as a powerful vasoconstrictor. It also contributes to the maintenance of fluid-electrolyte balance. The importance of AgII is not limited to its physiological regulatory functions; it is also evaluated as a biomarker in various cardiovascular and metabolic diseases. In clinical conditions such as hypertension, heart failure and chronic kidney disease, the observation of increased AgII levels in plasma or urine provides important clues about the underlying physiological processes of these diseases. In this context, measuring AgII levels provides valuable information for diagnosing these diseases in the early stages and monitoring the course of the disease. This study aims to develop molecularly imprinted nanoparticle-based surface plasmon resonance (SPR) sensors for the detection of AgII from human serum. To achieve this, AgII-imprinted (AgII-MIP) and non-imprinted nanoparticles (NIP) were synthesized using the molecular imprinting method. The synthesized nanoparticles underwent detailed analysis through Zeta-size measurements, Transmission Electron Microscopy (TEM), Scanning Electron Microscopy (SEM), and FTIR spectroscopy techniques. According to the data obtained from Zeta-size measurements, the particle sizes of AgII-MIP and NIP nanoparticles were determined as 46.51 nm and 48.97 nm, respectively. The nanoparticles were then used to coat the surface of the SPR chip. Thus, SPR chips coated with AgII-MIP nanoparticles (AgII-MICspr) and NIP nanoparticles (NICspr) were successfully obtained. Characterization studies of the chips were carried out by Contact Angle and Atomic Force Microscopy. AgII solutions were made at a range of

concentrations (3-100 pg/mL) and these solutions were interacted with the AgII-MICspr chip. The AgII-MICspr chip showed sensitive detection ability even for very low AgII concentration (3 pg/mL). In addition, selectivity studies were performed using AgII-MICspr and NICspr chips. Here, Angiotensin I (AgI) and vasopressin (Vp) were used as competitors. It was determined that the selectivity of the AgII-MICspr chip against AgII was 4.75 and 5.43 times higher than AgI and Vp molecules, respectively. Reusability studies were performed using the AgII-MICspr chip and it was observed that the chip preserved its functionality in the binding regions even after 10 repetitions. AgII detection studies were conducted from human serum. The chip was able to selectively detect very low concentrations of AgII even in this complex environment.

Keywords: Angiotensin II, Molecular imprinting technique, SPR sensor, Human serum.

Dedication

I wholeheartedly dedicate this thesis to my beloved mother, who has always been by my side with her endless love, sacrifices and unending support.

ACKNOWLEDGEMENTS

First of all, I would like to express my deepest gratitude to my valuable supervisor, Prof. Gözde BAYDEMİR PEŞİNT, who was with me with her smiling face, compassion, endless support and guidance throughout my doctoral education. Her expertise in her field, constructive feedback and encouraging attitude made a huge impact on my academic development. I am grateful to her for all the opportunities she has provided me and the knowledge she has imparted to me.

I would also like to thank my dear friends Okan ZENGER, Burcu EREN YÜNGEVİŞ and Pırıl ARISOY for their support under all circumstances, their help, and for creating a warm and pleasant working environment. I feel very lucky to have such a team.

I would like to express my sincere gratitude to my family, especially my mother Fatma CEMEK, who devoted her whole life to the happiness and education of her children and always dreamed of a beautiful future for them. My dear mother, who contributed the most to me reaching this day, I can never repay you for what you have done to me. I hope this thesis can show, at least to some extent, that your efforts were not in vain and how valuable your belief in me has always been.

I would like to thank my dear brother Mevlüt Türk CEMEK and sister Buse CEMEK, whose love and support I feel most deeply and who always motivate me.

I would like to express my deepest gratitude to my dear husband Emre Coşkun ŞAHİN, who makes my heart warm, who holds my hands when I am tired and gets me back on my feet, and who always makes me feel his love, compassion and support. Your presence gave me strength and courage on this journey. I am grateful to you for being by my side at every moment and for supporting me with your patience and understanding. Thank you endlessly, my darling, for making my life more beautiful and meaningful.

I would like to thank my dear daughter İdil Doğa ŞAHİN, who made me a mother and made me experience the purest form of love, for adding meaning to my life with her existence.
This thesis study was financially supported by TÜBİTAK within the scope of project number 220Z052.

TABLE OF CONTENTS

LIST OF FIGURES

LIST OF TABLES

LIST OF ABBREVIATIONS

RAAS	: Renin-Angiotensin-Aldosterone System
AgII	: Angiotensin II
AgI	: Angiotensin I
Vp	: Vasopressin
ACE	: Angiotensin Converting Enzyme
MIP	: Molecularly Imprinted Polymer
NIP	: Non Imprinted Polymer
PVA	: Polyvinyl Alcohol
SDS	: Sodium Dodecyl Sulfate
VIM	: 1-Vinylimidazole
EGDMA	: Ethylene Glycol Dimethacrylate
HEMA	: 2-Hydroxyethyl Methacrylate
APS	: Ammonium Persulfate
PBS	: Phosphate Buffered Saline
TEM	: Transmission Electron Microscope
SEM	: Scanning Electron Microscope
FTIR	: Fourier Transform Infrared Spectroscopy
AFM	: Atomic Force Microscope
SPR	: Surface Plasmon Resonance
LOD	: Limit of Detection
AgII-MICspr	: SPR chip coated with AgII-MIP nanoparticles
NICspr	: SPR chip coated with NIP nanoparticles
Cspr	: Non-coated SPR chip

LIST OF SYMBOLS

mg	: Milligram
ng	: Nanogram
pg	: Picogram
L	: Liter
mL	: Milliliter
µL	: Microliter
nm	: Nanometer
min	: Minute
h	: Hour
mM	: Millimolar
T	: Temperature
°C	: Celsius degree
ΔR	: Delta reflection
R_{max}	: Maximum SPR signal shift
Ka	: Association constant
Kd	: Dissociation constant
C	: AgII concentration
1/n	: Freundlich surface heterogeneity index
k	: Selectivity coefficient
k′	: Relative selectivity coefficient

1. INTRODUCTION

The importance of the Renin-Angiotensin-Aldosterone system (RAAS) in modulating blood pressure, electrolyte balance and vascular development is well known. Chronic disorders such as coronary heart disease, hypertension, chronic renal failure and diabetes are often associated with excessive RAAS activation (Şerbetçi and Boğa, 2022). Angiotensin II (AgII) is an octapeptide of the RAAS. It is formed by the conversion of Angiotensin I (AgI), which is formed as a result of the breakdown of angiotensinogen by renin released from the kidney, to AgII by the angiotensin converting enzyme (ACE). It is a powerful vasoconstrictor. It is essential for the regulation of blood pressure and the maintenance of water and electrolyte homeostasis. It helps to remodeling the heart and veins by affecting the heart and blood vessels. In addition, AgII acts as a growth factor and stimulator of various pro-inflammatory cytokines (TNF-α, interleukin-6). It shows its physiological effects through a series of receptors, especially the AgI receptor (Gard, 2002; Cheng et al., 2005; Sriramula et al., 2008; Busse et al., 2017).

Recently, a significant increase has been observed in the number of studies using optical sensors to measure physical, chemical and biological properties. Surface plasmon resonance (SPR) is an optical technique that monitors changes in refractive index (RI) on the sensor surface and does not require the use of labels to characterize macromolecular interactions. In this method, a thin metal film consisting of gold or silver is used between two media with different refractive indices. When P-polarized light passes from a medium of high optical density to a medium of lower density, full reflection occurs if the incidence angle of the radiation is greater than the critical value. As a result of this event, a temporary wave is formed in the medium with low density. This wave interacts with the free electrons on the metal surface, reducing the intensity of the reflected light. This event is called SPR (Englebienne et al., 2003; Kamal Eddin and Fen, 2020). SPR causes changes in the binding and RI between the analyte in solution and the analyte-specific ligand bound to the sensor surface. Compared to many devices commonly used in biochemical analysis, SPR-based sensors are versatile, easy to use, compatible with a wide variety of chemicals, and highly sensitive (McDonnell, 2001). However, it is sometimes not sufficient for sensitive detection of analytes at low concentrations. For this purpose, SPR sensors, which are integrated with

nanomaterials, have been promising for bio-sensing studies due to their high specificity (Kamal Eddin and Fen, 2020). In addition, SPR sensors are widely used in the examination of affinity-based interactions such as antibody-antigen, enzyme-substrate and ligand-receptor, and in the detection of drugs and biomarkers (Bellassai et al., 2019).

Molecular imprinting is a technique used in the synthesis of polymers containing specific recognition sites for the template molecule. It takes place in three basic steps; first, a pre-complex is formed between the template molecule and the appropriate functional monomer. The pre-complex is then polymerized by adding cross-linkers and monomers to the medium (Yıldırım and Baydemir Peşint, 2021). Following polymerization, desorption agents are utilized to extract the template molecule from the polymer structure. As a result, molecularly imprinted polymers (MIPs) are generated, featuring distinct recognition sites (Saylan et al., 2017). For molecular detection and identification applications, MIPs are appealing due to their selective binding qualities, robustness, and ease of production (Ding et al., 2020). MIP technology has considerably progressed over recent years as both an approach and a method that can be used in a wide variety of applications such as solid phase extraction, chemical reaction catalysis, chromatographic separation and biosensing (Li et al., 2019).

This study aimed to develop molecularly imprinted nanoparticle-based surface plasmon resonance (SPR) sensors for detecting AgII from human serum. To achieve this, AgII nanoparticles were synthesized using the molecular imprinting method and comprehensively characterized. These synthesized nanoparticles were then used to coat the surface of an SPR chip. The characterization of the fabricated chips was performed. Additionally, the efficiency to detect AgII at various concentrations, the selectivity to bind AgII over other molecules, and the ability to detect AgII from human serum were evaluated. AgII acts as a biomarker in the identification of multiple medical conditions such as high blood pressure, cardiovascular diseases, and COVID-19 infection. According to the literature, for the detection of AgII, long-time and labor-intensive methods such as High-Performance Liquid Chromatography (HPLC), UV-spectrophotometer, Immuno-Matrix Assisted Laser Desorption/Ionization are used. In addition, some of these methods used do not have sufficient sensitivity. Our study will be a pioneer in the literature in terms of developing SPR sensor systems integrated with molecular imprinting technology for rapid, sensitive and specific detection of AgII.

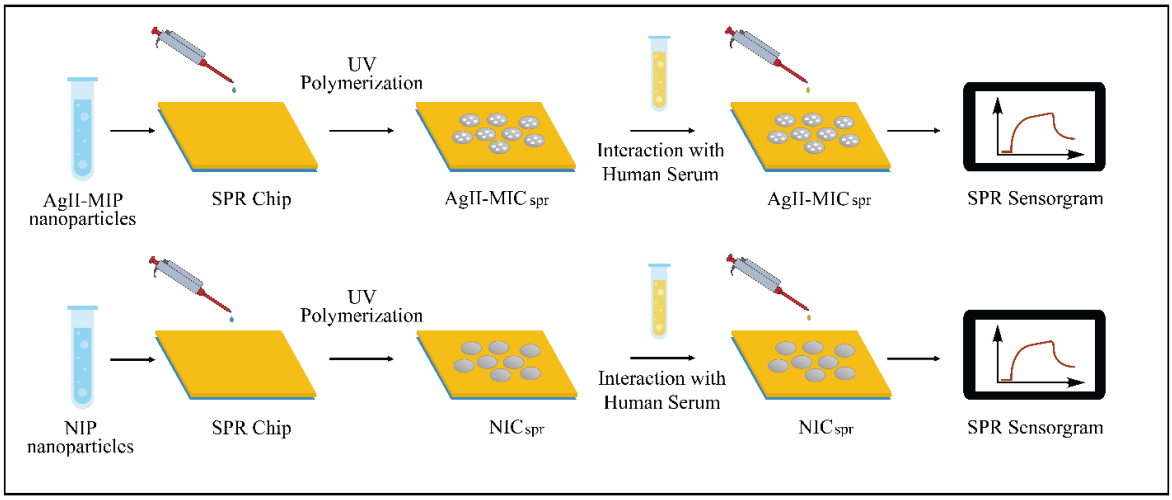

Figure 1.1. General summary of the study.

2. THEORETICAL FOUNDATIONS AND LITERATURE REVIEW

2.1. Renin-Angiotensin-Aldosterone System (RAAS)

The RAAS is a crucial hormonal cascade that modulates blood pressure, electrolyte balance, and fluid volume in the body. This intricate system involves the coordinated actions of renin, angiotensin, and aldosterone, each playing a vital role in maintaining physiological equilibrium. The RAAS exerts its effects through a series of processes that involve vasoconstriction, renal sodium retention, and pro-inflammatory and oxidative actions that can lead to endothelial dysfunction, microalbuminuria, and insulin resistance (Volpe et al., 2012).

Renin, generated in the kidneys, initiates the RAAS cascade by cleaving angiotensinogen to form AgI. AgI is then converted to AgII by ACE, a key step in the system that leads to vasoconstriction and aldosterone release (Patel et al., 2017). AgII acts on blood vessels to increase blood pressure and triggers the suprarenal glands to release aldosterone, a hormone that regulates sodium/potassium balance (Morishita and Kusano, 2013). Aldosterone promotes sodium reabsorption in the kidneys, leading to increased blood volume and blood (Poulsen and Fenton, 2019)

The RAAS plays pivotal roles in various physiological processes, including the pathogenesis of chronic kidney disease, hypertension, and cardiovascular diseases (Faria-Silva et al., 2005). The system's dysregulation can result in electrolyte imbalances, volume overload, and hypertension (Lamb and Folstad, 2003). The balance between the components of the RAAS is critical for maintaining homeostasis and responding to changes in sodium intake, blood pressure, and fluid status (Hayden et al., 2012).

Some studies have highlighted the role of the RAAS in modulating endothelial function, vascular tone and renal fibrogenesis (Lindpaintner et al., 1990). The system's activation can lead to the development of conditions like atherosclerosis and nephrosclerosis, emphasizing its impact on cardiovascular health (Meretskyi et al., 2017). Understanding the intricate regulatory mechanisms within the RAAS is essential for developing targeted therapeutic interventions for conditions influenced by RAAS dysregulation (Lillyblad et al., 2012).

2.2. Angiotensin II (AgII) and Its Effect on Health

AgII, a key component of the RAAS, is a bioactive peptide with significant implications for health. This peptide is produced by the cleavage of angiotensinogen by renin to form AgI, which is then converted to AgII by ACE. AgII interacts with specific receptors, namely type 1 (AgII-T1) and type 2 (AgII-T2), playing significant roles in various physiological processes (Al-Bayati and Al-Nahi, 2022). AgII affects cardiovascular function and renal physiology by inducing vasoconstriction, sodium retention, and aldosterone release, particularly by acting through the AgII-T1 (Zhang et al., 2020). AgII contributes to oxidative stress and inflammation, which are other important factors in cardiovascular pathologies (Fuloria et al., 2022). It is also associated with adverse left ventricular remodeling and myocardial injury responses. This highlights the importance of AgII in cardiac function and pathology (Mascolo et al., 2021).

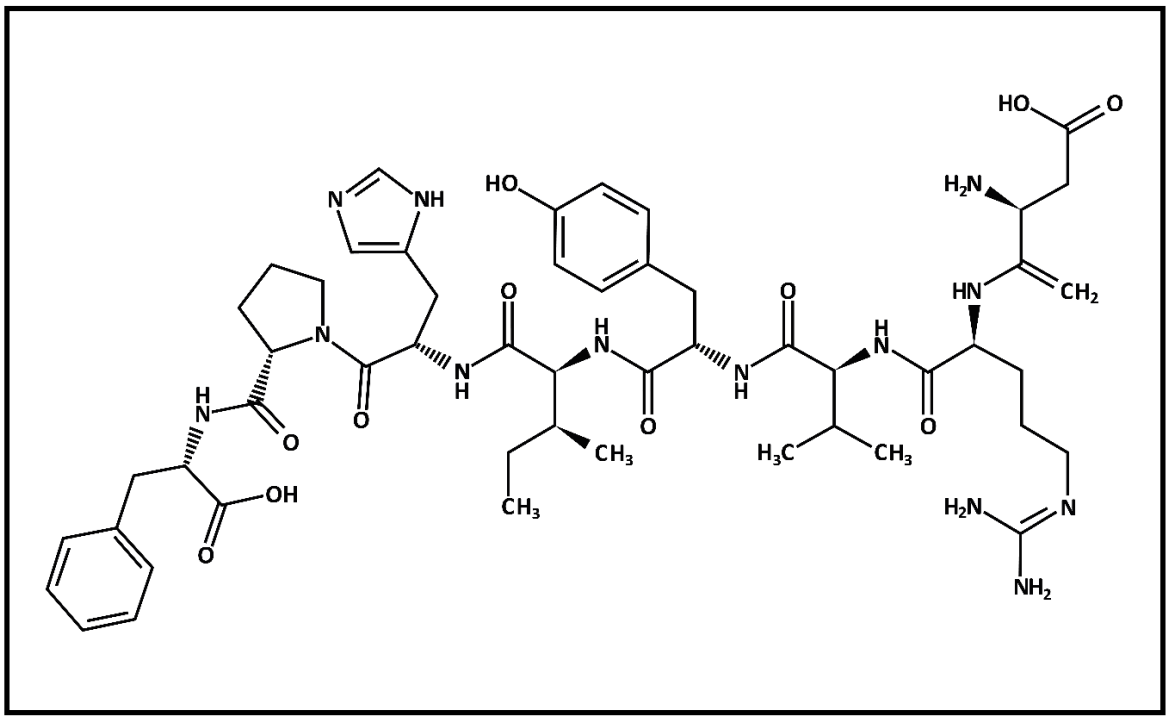

Figure 2.1. AgII chemical structure.

Also, AgII has been associated with viral infections, with angiotensin-converting enzyme 2 (ACE2) acting as a negative regulator that reduces AgII levels, thereby influencing the balance of the renin-angiotensin system (RAS) (Liu et al., 2020). The conversion of AgII to Ag-(1–7) by ACE2 has been shown to counteract the negative effects of the RAS,

highlighting the regulatory role of AgII in maintaining physiological balance (Ni et al., 2020). Additionally, AgII has been shown to be involved in modulating myeloid signaling in sepsis, enhancing bacterial clearance, and influencing the systemic inflammatory response (Leisman et al., 2022). Moreover, AgII has been linked to vascular hypertrophy, fibrosis, inflammation, and oxidative stress. Interventions such as neohesperidin have shown promise in attenuating AgII-induced vascular remodeling (Zhang et al., 2022).

AgII is known to activate many signaling pathways, including phosphoinositide conversion and calcium mobilization, as well as activation of glycogen phosphorylase and adenylate cyclase through AgII-T1 receptors (Chhabra et al., 2013). Studies have also shown that it inhibits insulin-stimulated phosphorylation of eukaryotic initiation factor 4E binding protein-1, so interfering with insulin signaling and protein synthesis (Duraisamy et al., 2001). AgII can modulate the expression of various factors such as Cbfa1 and RANKL via the cAMP signaling pathway, which may have effects in conditions such as hypertension-related osteoporosis (Guan et al., 2011). AgII has also been shown to stimulate nitric oxide production in the pulmonary endothelium via the AgII-T2 receptor, while signaling via the AgII-T1 receptor negatively regulates nitric oxide production (Olson et al., 2004).

AgII serves as a biomarker for diagnosing multiple illnesses, among them COVID-19. Studies on COVID-19, especially in recent years, have shown that high AgII levels are observed in critically ill COVID-19 patients, and RAAS dysregulation, characterized by altered AgII levels, has been associated with serious consequences in COVID-19. It emphasized the importance of monitoring the AgII level to assess the intensity of the illness and the individual's reaction to treatment and demonstrated the potential of AgII as a prognostic indicator (Camargo et al., 2022; Meng et al., 2020). Other studies on this subject have shown that AgII levels may be affected by antihypertensive drugs such as ACE inhibitors (ACE-Is) and AgII receptor blockers (AgII-RBs). The results of the studies have revealed that these drugs have healing potential in COVID-19 patients (Rocheleau et al., 2022).

Detecting AgII levels is crucial to comprehending its contribution in various physiological processes and disease conditions. Several techniques and tools have been created to detect AgII, each presenting distinct advantages and limitations. A notable method for AgII

detection is liquid chromatography-electrospray ionization-tandem mass spectrometry (LC-ESI-MS/MS). This technique allows precise measurement of AgII levels in biological samples. Nevertheless, LC-ESI-MS/MS requires specialized equipment and expertise, which may hinder its widespread use in routine clinical settings. Another approach to AgII detection involves immunoaffinity purification using anti-AgII antibodies. This method facilitates the isolation and quantification of endogenous AgII in plasma samples, providing a reliable tool for assessing hormone levels. However, the fact that this technique is time-consuming and labor-intensive limits its use for high-throughput analyses (Schulz et al., 2014). Aside from mass spectrometry and immunoaffinity purification, capillary electrophoresis coupled with UV and electrochemical detection has been employed for AgII detection. This method provides enhanced detection limits and sensitivity, facilitating the efficient extraction and quantification of AgII. Nevertheless, difficulties arise in optimizing separation conditions and ensuring reproducibility in complex biological samples (Lacher et al., 2002). Another technique for detecting AgII is HPLC. However, this method can sometimes present challenges in obtaining precise and accurate measurements of AgII. Additionally, the sample preparation and analysis process for HPLC can be time-consuming (Popp et al., 2017). UV spectrophotometry is also used for AgII detection, but this technique struggles with the specific identification of AgII amidst other molecules in the sample and lacks the sensitivity required to detect low concentrations of AgII (Shi et al., 2022). Immuno-Matrix Assisted Laser Desorption/Ionization (IMALDI) is a technique used to detect AgII. This technique enables highly sensitive and specific detection of AgII. However, issues with nonspecificity and long analysis times in immunoassays can impact both accuracy and efficiency (Popp et al., 2017).

2.3. Biosensors

Biosensors are instruments that use components responsible for biological sensing to convert changes occurring in a reaction into comprehensible signals (electrical/optical/mass change). These components include diverse options such as DNA, aptamer, antibody, enzyme and cell. Interactions between a targeted molecule and these components are converted into intelligible signals by a sensor equipment called a transducer (Liu et al., 2014; Karunakaran et al., 2015; Mehrotra, 2016). It was first invented by Clark and Lyons in 1962 for the electrochemical detection of oxygen or hydrogen peroxide with an immobilized glucose oxidase electrode for

the measurement of glucose from biological samples. Since then, great advances have been made in technology and biosensor applications, including innovative approaches such as electrochemistry, nanotechnology and bioelectronics (Vigneshvar et al., 2016).

In the sensing process of a biosensor, receptors accountable for biological sensing, transducers signaling alterations, and electronics displaying these signals play integral roles. Designing biosensors that provide accurate and reliable results, can be used repeatedly, and remain stable even when different parameters are adjusted is very important for all applications in which they will be used. They find extensive utilization across diverse application domains, encompassing diagnostic applications, screening for contaminant and pesticides, as well as research into factors contributing to ecological pollution (Yuan and Liu, 2021; Sharma et al., 2025).

Biosensors can be divided according to the kind of energy transfer occurring within the transducer as;

- Thermal,
- Electrochemical,
- Magnetic,
- Optical,
- Colorimetric,
- Gravimetric
- Piezoelectric biosensors

Alternatively, categorization can occur depending on the type of bioreceptor as;

- Nucleic acid,
- Enzyme,
- Aptamer,
- Antibody
- Cell biosensors (Perumal and Hashim, 2014).

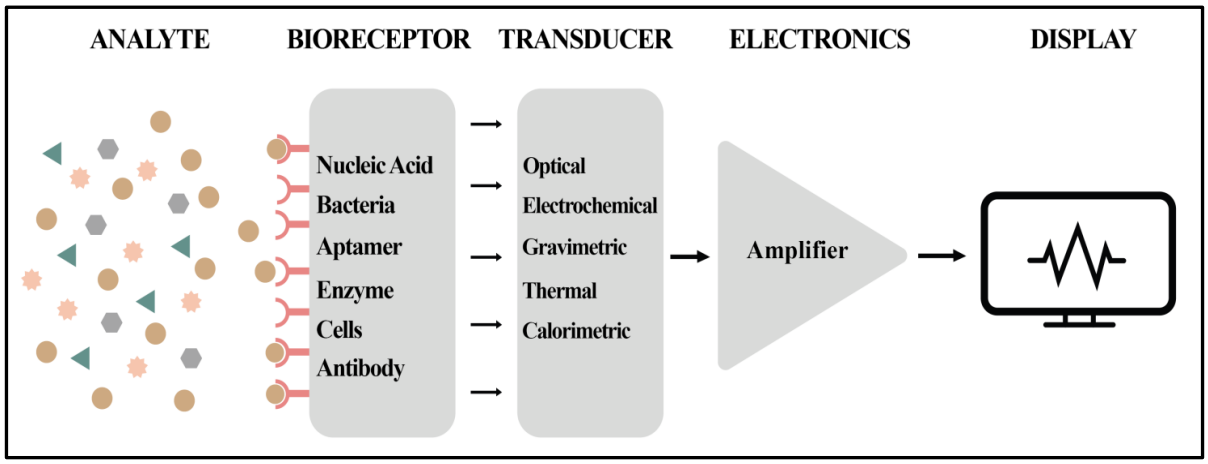

Figure 2.2. Main components of a biosensor.

Biosensors offer striking advantages over traditional methods. Traditional methods are generally require time-consuming preparation steps, need proficient users, and use large amounts of sample. In contrast, biosensors stand out with features such as easy portability, simple and convenient design, and real-time target molecule detection. Besides these advantages, it may also have disadvantages such as low stability in the long term, detection of only one target molecule, and limited mercantile use (Mehrvar and Abdi, 2004; Van Dorst et al., 2010).

2.3.1. Optical Biosensors

These are sensors in which the interaction of the target with the bioreceptor is detected with the help of an optical-based transducer. The optical converter performs analyzes using properties of light such as absorption, scintillation, reflection and refraction. There are optical biosensor systems that work with two different methods: labeled and label-free. Labeled method is the method in which the analyte and bioreceptor are labeled with some labels that can help in detection. Label-free method is the method in which detection is carried out directly, without the need for any labels. It allows analyzes to be made quickly and without difficulty. Optical biosensor systems include advantages such as strong signal, direct and fast detection. It has a broad spectrum of uses, spanning from healthcare to defense sectors. The most commonly used optical-based sensing is surface plasmon resonance (SPR). Here, interactions are determined by monitoring the behavior of light sent to the metal surface (Perumal and Hashim, 2014; Damborský et al., 2016; Gundogdu et al., 2023).

2.3.1.1. Surface Plasmon Resonance (SPR)

Surface Plasmon Resonance (SPR) is an advanced sensing technology that allows the real-time detection of various molecules. In this method, the refractive index (RI) of the surface changes as a result of the interaction between the target molecule to be detected in a solution and the selective ligand anchored to the sensor surface. This change is measured with high sensitivity by the SPR device, and the binding event is analyzed quantitatively and qualitatively. Thus, intermolecular interactions can be monitored in a non-labeled, fast and dynamic way (Capelli et al., 2023).

SPR is founded on the principle of surface plasmon excitation resulting from the interaction between a metal surface (typically gold) and a dielectric medium (a liquid sample) at their interface. In the SPR system, when light is sent to a metal surface at a certain angle (resonance angle), this angle is determined only by the RI of the medium that the metal is in contact with. When the medium changes, the RI changes proportionally and this affects the interaction of light with the surface. Even this small change causes a shift in the resonance angle (Homola, 2008). This shift is measured by optical detectors and provides information about the kinetic and thermodynamic parameters of the binding processes. In this way, the

binding and dissociation rates of molecules and the interaction affinity can be calculated (Rich and Myszka, 2000).

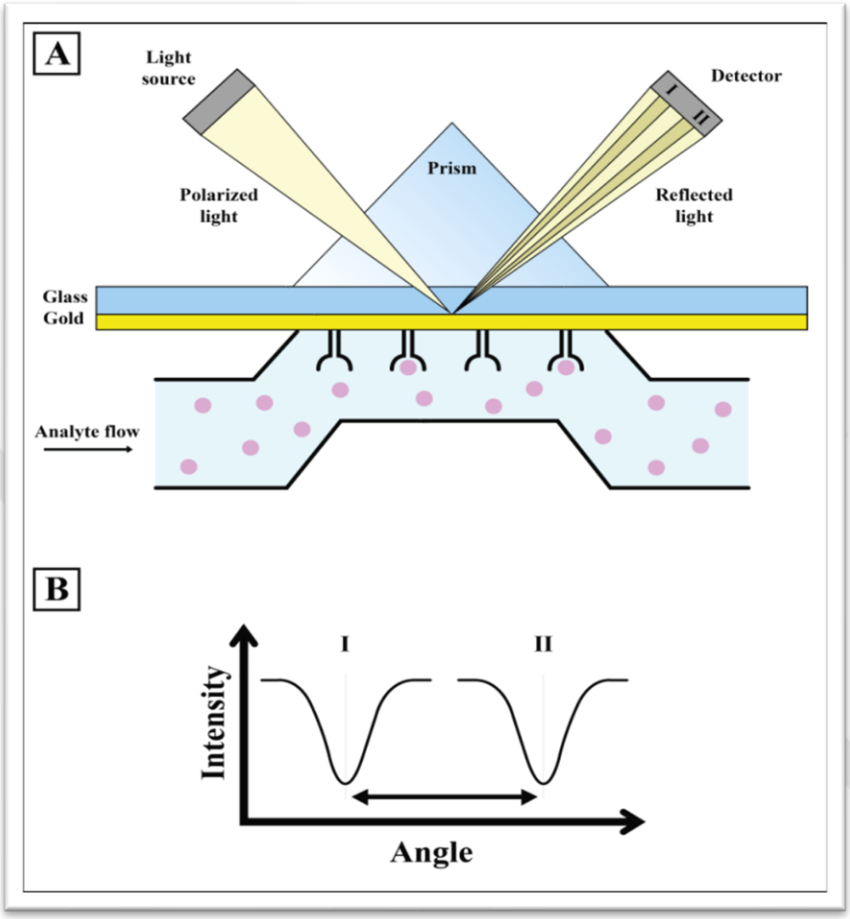

Figure 2.3. A) Operating principle diagram of SPR-based sensor, B) Resonance angle change.

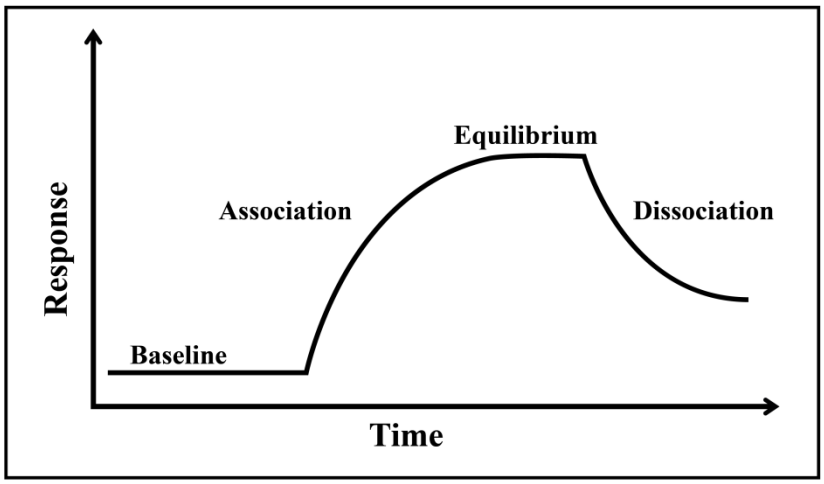

Figure 2.4. Graphical display of interaction kinetics monitored via SPR.

The SPR technique allows reliable results to be obtained even in complex biological samples, since other components in the sample do not have a significant interference effect on the analysis. Thanks to this feature, the need for prior purification or processing of samples is largely eliminated. It also offers a significant advantage, especially when working with rare or valuable samples, as only a tiny quantity of sample suffices for analysis. The absence of the need for labeling simplifies the analysis process and increases efficiency in terms of time and cost (Capelli et al., 2023).

Many studies have been carried out on surface plasmons since the early 1900s. A scientist named Wood observed in a study that some spectra of the light transmitted through a metal grating were not visible, but he was later able to explain this phenomenon with Rayleigh theory. Another scientist named Sommerfeld was able to partially explain the meaning of the electromagnetic waves occurring on the grid surface with his experiments, but he could not determine that these were SPR. This process continued with many discoveries and contributions until the end of the 1900s. With the development of SPR technologies and SPR devices between 1980 and 1990, surface plasmons began to find application areas (Chen et al., 2023).

One of the most important factors in the design of devices working with SPR theory is the light source used. This light source has a major impact on the design of devices and the ability to detect the sample in real time. The production and use of more compact, high detection ability and easily portable light sources have made significant contributions to the

development of SPR technology (Prabowo et al., 2018). Another important factor for these devices is the choice of metals used. Various metals such as gold, silver, titanium, copper, and aluminum can be employed. Certain properties of these metals (such as chemical stability, sharp resonance, and cost-effectiveness) necessitate careful selection. Gold is the primarily preferred and used metal because it is inert, induces a strong SPR signal, and is easy to work with. Additionally, various molecules can be easily immobilized onto the gold surface modified with mercaptan. Conversely, alternative metals are less preferred due to specific drawbacks: silver oxidizes easily, titanium has a high cost, and aluminum is not highly responsive to variations in the RI of the target molecule. RI alterations occurring on the surface of metal can change the angle and wavelength of light sent to the surface of metal, as well as the light intensity reflected from the surface of metal. This amount of variation depends on the RI alterations of the environment in which the surface of metal is located. SPR has become a widely utilized method today because it allows the analysis of numerous samples in various physical phases (Abdulhalim et al., 2008).

2.3.1.2. SPR Biosensors

SPR biosensors constitute a commonly applied class of optical-based biosensors and have the ability to detect molecules with high sensitivity without labels. They consist of an optical component that excites surface plasmons and establishes resonance conditions, along with target-specific binding agents. These binding agents (e.g. antibodies, aptamers, or molecularly imprinted polymers) are immobilized on a metal layer (commonly gold) and allow specific interactions to occur. Thus, molecular bindings can be detected with high accuracy via refractive index changes on the sensor surface (Ravindran et al., 2023).

SPR biosensors not only offer high sensitivity and specificity but also provide rapid, real-time, and non-labeled detection capabilities (Das et al., 2023; Park et al., 2022; Herrera-Domínguez et al., 2023). Compared to other optical biosensing techniques, they demonstrate superior performance in achieving low detection limits (Herrera-Domínguez et al., 2023). Furthermore, their minimal sample preparation and short measurement times make them highly suitable for point-of-care (PoC) applications (Das et al., 2023). Recent advancements in SPR biosensor technology include the integration of nanomaterials to enhance both performance and selectivity (Park et al., 2022).

SPR biosensors have diverse applications in biomedical research, food testing, proteomics, and drug research (Willander and Al-Hilli, 2009). They are used for detecting biological analytes, DNA hybridization, virus diagnosis, enzyme-substrate interactions, antibody characterization, and protein conformation studies. They can analyze a wide range of analytes, from small organic molecules to large protein complexes (Ramanavièius et al., 2005). SPR biosensors have been successfully applied in clinical diagnostics, food quality control and environmental surveillance, detecting biomarkers, hormones, antibodies, endocrine disruptors, pathogens, and toxins (Homola, 2009).

SPR biosensors are widely used for the detection of specific biomarkers (e.g., proteins and nucleic acids) associated with a wide range of health problems, ranging from cancer to infectious diseases. These highly sensitive systems make it possible to diagnose diseases at early stages. In addition, they enable the analysis of biomarkers that reflect the response to treatment, contributing to the development of targeted treatment strategies appropriate to the molecular profile of individuals. In this respect, they increase the applicability of personalized medicine and contribute significantly to the expansion of patient-centered health services (Butt, 2025).

The pharmaceutical industry extensively utilizes SPR-based biosensing technologies to perform detailed analyses of molecular-level interactions throughout drug discovery and development processes. This technology enables real-time and label-free investigation of binding events between drug candidates and biological targets, as well as antibody-antigen recognition and receptor-ligand interactions. The kinetic parameters of these interactions—such as association and dissociation rates, and binding affinities—provide critical insights into the efficacy, selectivity, and safety profiles of drug compounds. SPR systems allow for rapid and highly accurate characterization of such molecular interactions, facilitating the screening and ranking of potential drug candidates. Consequently, SPR contributes to enhanced research and development efficiency by significantly reducing both the time and cost associated with the drug discovery and development process (Butt, 2025).

In addition, SPR biosensors are effectively used in the detection of heavy metals (e.g. lead, mercury and cadmium), pesticides and various organic and inorganic pollutants found in

nature. These biosensors also serve as a powerful control tool to monitor compliance with environmental regulations and quality standards. They are widely used in the detection of microbial contaminants (e.g. E. coli, Salmonella spp.) and hazardous chemicals, especially in drinking water and wastewater systems. These systems, which offer real-time analysis, enable rapid intervention by identifying potential environmental hazards at an early stage (Çaktü Güler et al., 2024; Butt, 2025).

SPR biosensors also serve as a valuable tool for upholding food hygiene and quality standards. These sensors have the capacity to detect harmful substances, microbial spoilage and allergy-causing substances in food composition quickly and with high sensitivity. SPR-based systems, which provide results in a shorter time compared to traditional analysis techniques, offer instant control in the food production process (Ansari et al., 2023).

2.4. Molecular Imprinting Technique

Molecular imprinting is a technology inspired by the “lock-key” relationship between enzyme and substrate. Its history dates back to the 1930s when Polyakov first developed the concept. He utilized aromatic hydrocarbons as template molecules and established the foundations of the technology by creating a silica gel that surrounded these hydrocarbons. Polyakov's breakthrough sparked a surge of research in this field, with numerous scientists have conducted similar investigations employing a variety of template molecules (Chen et al., 2011; Sajini and Mathew, 2021).

The molecular imprinting technique (MIT) is a technique utilized for the fabrication of molecularly imprinted polymers (MIPs), endowed with specific recognition sites. These sites are meticulously tailored to fit the shape, size, and functional groups of the template (Chen et al., 2016; Saylan et al., 2019). This technology facilitates the creation of synthetic receptors with predetermined selectivity and specificity, rendering them highly suitable for diverse applications (Vasapollo et al., 2011). The initial stage of this technique involves the formation of a pre-complex between the template molecule and functional monomer through covalent or non-covalent interactions. Subsequently, polymerization takes place using a crosslinker, monomer, and pore-forming solvents selected based on the template molecule. Following polymerization, the template molecule is extracted from the polymeric structure using

appropriate solvents. This process yields polymeric materials containing cavities tailored to the shape and dimension of the template molecule. These cavities exhibit selective binding towards target species that share structural and chemical similarities with the template molecule (Akgönüllü et al., 2023). MIT has evolved into a versatile and interdisciplinary domain through the amalgamation of materials chemistry, polymer chemistry, biochemistry, and numerous other fields (Liu et al., 2019).

The cost-effectiveness of this technique and the simplicity of its production process, along with the durable and stable structure of the resulting polymer, render it a more favorable choice compared to traditional methods such as monoclonal antibodies (Li et al., 2016; Motamedi et al., 2022). MIT has been effectively employed in many areas, from biosensors to environmental analysis, from drug delivery to chromatography. The wide usage area and effectiveness of this method are frequently emphasized in the literature (Ertürk and Mattìasson, 2017).

Furthermore, MIT has been instrumental in creating advanced synthetic support structures (like scaffolds) for cell adhesion and proliferation, demonstrating its potential in tissue engineering applications (Algieri et al., 2014). By incorporating molecular affinity sites into polymeric matrices, MIT provides a powerful tool for creating artificial recognition sites with specific binding abilities, offering a versatile and effective approach for molecular recognition (Saylan et al., 2017).

2.4.1. Polymer Synthesis Processes using Molecular Imprinting Technique

MIPs are synthetic materials created with recognition sites that match the functional groups, shape and dimension of target (analyte) molecules. These polymers are crafted using a method called “molecular imprinting”, where the target molecule is employed to form voids within the polymer composition. These voids exhibit selective binding to the target molecule, demonstrating strong affinity and specificity (Zuo et al., 2022).

Its remarkable selectivity and specificity towards the target molecule offer a significant advantage in the imprinting process. These characteristics render them invaluable in diverse fields including biosensor applications, separation, purification, environmental remediation, and drug delivery (Gao et al., 2020; Zare et al., 2022). Their robust and enduring structure,

coupled with their reusability, positions them as cost-effective and eco-friendly alternatives compared to numerous other methods (Lu et al., 2022). The capacity to discern the target molecule amidst environments comprising various components enhances desired attributes like accuracy and sensitivity in analytical methods (Takahashi et al., 2022).

Although MIPs are synthesized using various imprinting techniques, all of them incorporate the following three common processes (**Figure 2.5.**):

I. A structure known as a pre-complex is formed through the covalent or non-covalent interaction between a molecule identified as the target and a functional monomer.
II. By using cross-linking agents, monomers and molecules that initiate the polymerization process, a polymer network surrounding the pre-complex structure is formed.
III. The analyte (template/target) is extracted from the resulting polymeric structure and voids are created in the structure that recognize the template and allow it to facilitate reattach (BelBruno, 2018).

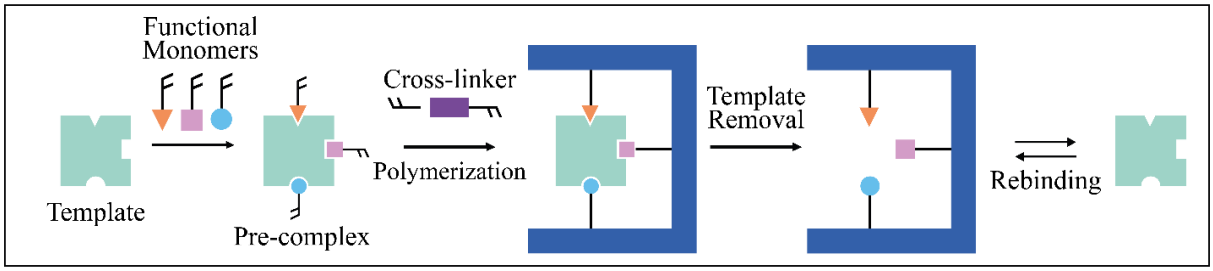

Figure 2.5. Molecular imprinting process.

2.4.2. Imprinting Approaches Used in the Synthesis of MIP

MIP synthesis is performed using covalent, non-covalent, and semi-covalent imprinting methods, depending on the types of interactions between the analyte and functional monomer during the polymerization and adsorption processes (Qi et al., 2010).

2.4.2.1. Covalent Interaction-Based Imprinting

Covalent imprinting is a molecular imprinting technique where functional monomers are covalently linked to template molecules during the imprinting process (Kalecki et al., 2023 ; Manickam et al., 2017). This method creates strong covalent linkages between template

molecules and functional monomers, leading to the formation of highly specific and stable recognition sites inside the polymer matrix (Mostafa et al., 2021). This method helps to increase specificity to the target molecule and reduce non-specific binding by ensuring the formation of homogeneous binding sites in the polymeric structure (Zhu et al., 2021). Moreover, it can prevent the leakage of the template molecule from the polymeric structure and increase the stability of the imprinted cavities (Zhang et al., 2020). Boronic ester bonds, Schiff base bonds and acetal bonds can be given as examples of the interactions that occur during this imprinting method. In order to obtain an extremely durable and hard polymer by covalent imprinting, extensive use of cross-linking agents can be seen (Sajini and Mathew, 2021). This method is less preferred since it is difficult to remove and reattach the template molecule from the polymeric structure formed after the printing process is completed (Chen et al., 2011).

2.4.2.2. Non-covalent Interaction-Based Imprinting

This imprinting method is based on the use of non-covalent interactions like hydrophobic or ionic interactions, dipole-dipole interactions and hydrogen bonds between the template molecule and functional monomer. However, weak non-covalent interactions between the template and the functional monomer may not be sufficient to form a complex structure. To acquire the complex structure, the amount of functional monomer must be increased. In the non-covalent imprinting method, it is easier to separate and reattach the template from the resulting polymer material compared to covalent imprinting. For this reason, polymers synthesized through non-covalent imprinting are primarily preferred in many applications, including HPLC and sensor applications. In this imprinting method, the most preferred functional monomer is methacrylic acid, capable of binding to different templates via hydrogen bonding, while EGDMA serves as the cross-linker (Zhang et al., 2006; Chen et al., 2011; Sajini and Mathew, 2021).

2.4.2.3. Semi-covalent Interaction-Based Imprinting

In this imprinting strategy, while polymerization occurs the template is attached to the functional monomer through covalent interactions. However, after removal from the polymeric structure, reconnection is achieved through non-covalent interactions. An intermediate group is used that facilitates the binding of the template molecule to the functional monomer. This group, functioning as a linker, is eliminated during the template's

reattachment to the polymer (Sajini and Mathew, 2021). The primary benefits of this approach are that it creates very homogeneous binding sites and has fewer non-specific binding sites compared to alternative imprinting approaches. In this way, polymers with enhanced selectivity and efficiency are created (Tan et al., 2016).

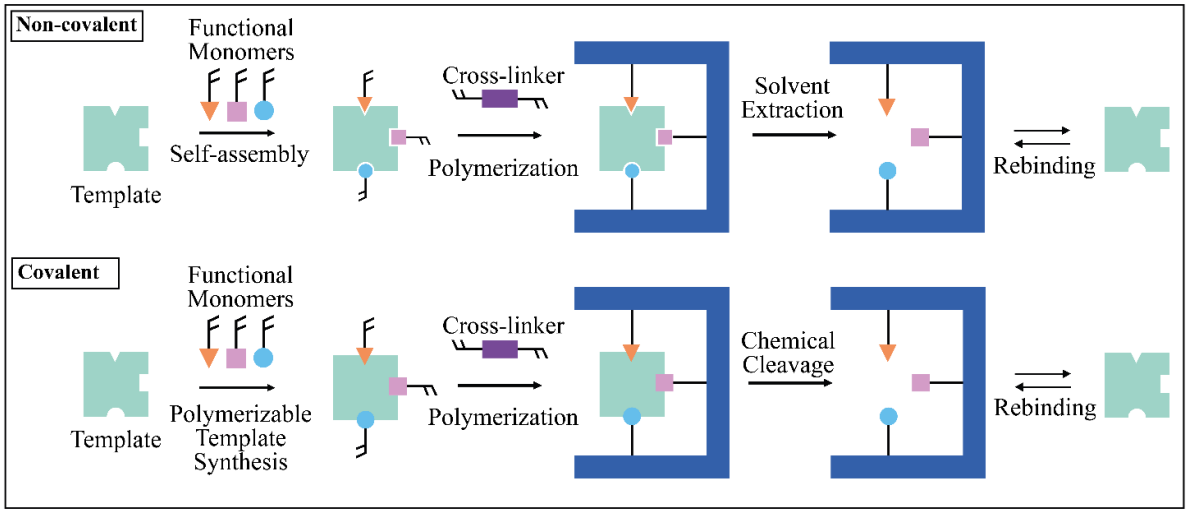

Figure 2.6. Visualization of imprinting approaches.

2.4.3. Essential Components Required for Synthesis of MIP

The manufacturing of MIPs necessitates the assembly of several essential components. These comprise a template (also called target or analyte) molecule, functional monomers, cross-linking agents, solvents (porogen), and initiators (Takeuchi and Matsui, 1996; Gong et al., 2004; Wang et al., 2012; Zink et al., 2018). Each component is explained in detail below:

2.4.3.1. Template (Analyte) Molecule

The tamplate molecule plays a key role in the imprinting proccess. It guides the interactions between groups that will engage with functional monomers. Template molecules should be chosen to be easily available at an affordable cost, and they should demonstrate high solubility, chemical, and thermal stability under the conditions of the imprinting process (Yan and Row, 2006; Sajini and Mathew, 2021). A wide variety of target molecules can be used as templates in molecular imprinting. However, not all target molecules are suitable for this method. Generally, templates with smaller molecular weights are preferred for MIP synthesis. Templates with larger molecular weights, such as cells, proteins, and various organic

compounds, can also be used, but synthesizing polymers with these molecules presents challenges. These include the difficulty of creating effective recognition sites within the polymeric structure due to the non-rigid nature of these larger molecules (Yan and Row, 2006).

2.4.3.2. Functional Monomers

These molecules collaborate with specific moieties on the target molecule, resulting in a pre-organized complex. This structure aids in the effective integration of the template molecule into the polymer matrix in subsequent stages. Hence, functional monomers are chosen to best interact with the target. These molecules ensure strong binding of the synthesized polymer to the target molecule, thus facilitating the successful synthesis of polymers through the molecular imprinting process (Chen et al., 2011; Hasanah et al., 2021; Sajini and Mathew, 2021). Functional monomers are generally categorized into three types: acidic monomers like acrylic acid, methacrylic acid, and itaconic acid; alkaline monomers such as 2-vinylpyridine, 4-vinylpyridine, and 1-vinylimidazole; and neutral monomers including styrene and 4-ethylstyrene. During the initial complexation step, the number of functional monomers should exceed the number of target molecules. This is to enhance the binding capacity for the target molecule. However, it is significant to carefully determine the amount of monomer, as an excess can lead to non-specific interactions (Hasanah et al., 2021).

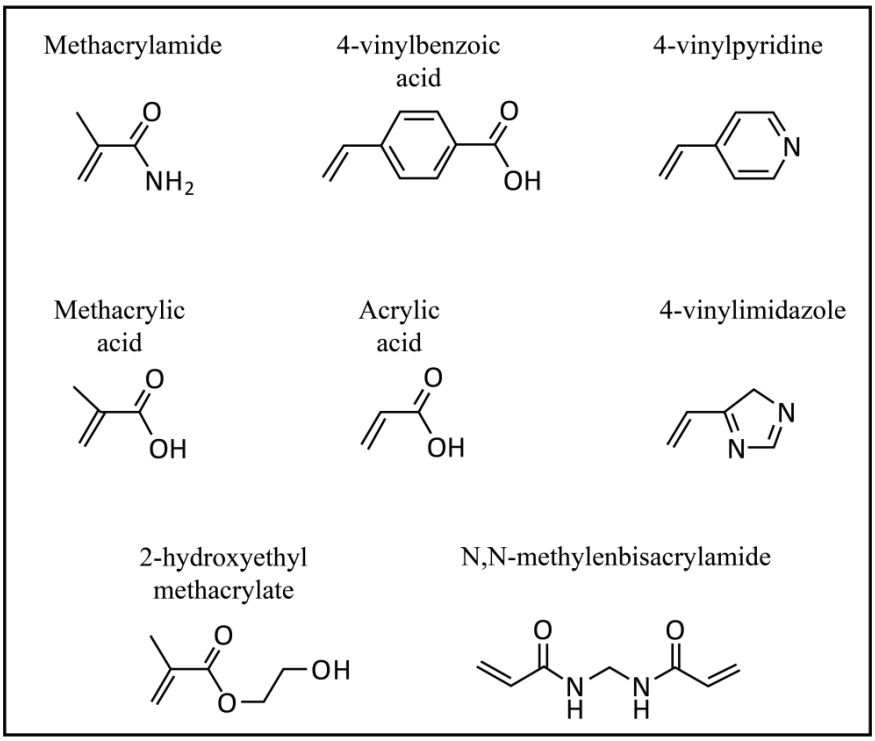

Figure 2.7. Certain functional monomers widely used in molecular imprinting applications.

2.4.3.3. Cross-Linking Agents

They, which help the template molecule to form a stable structure with the functional monomer through the polymerization process, enable the synthesis of hard and durable polymers containing a large number of cross-links. The presence of these agents significantly affects the morphological development of MIPs and contributes to the formation of well-defined and stable recognition sites. For the synthesis of porous and mechanically durable materials, many cross-links must be formed. In general, polymers with a cross-link ratio of 80% or more are widely used. In order for comonomers to be incorporated into the structure equally during the copolymerization process, the appropriate ratio of cross-linker/functional monomers must be determined (Cormack and Elorza, 2004).

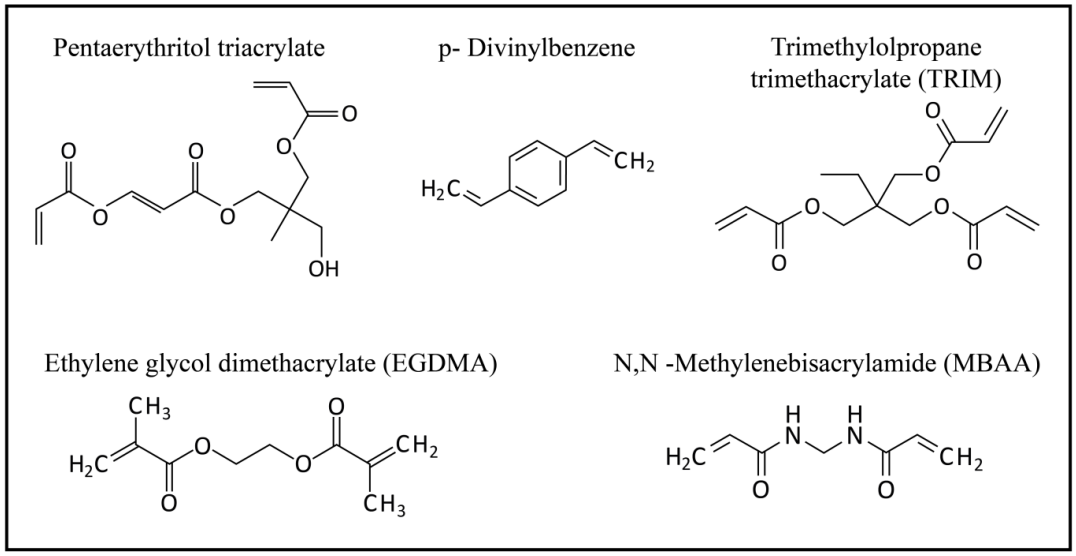

Figure 2.8. Certain cross-linkers widely used in molecular imprinting applications.

2.4.3.4. Polimerization Initiators

To initiate polymer synthesis using the free radical polymerization method, initiator molecules with diverse properties are employed to generate the necessary initiator radicals. These molecules are used in smaller quantities compared to the functional monomer in the imprinting process. They are activated by light, temperature, chemical, or electrochemical effects, transforming into radical monomers. For instance, azobisisobutyronitrile (AIBN), a commonly used initiator in MIP synthesis, decomposes via photolysis or thermolysis to produce carbon-based radicals (Yan and Row, 2006).

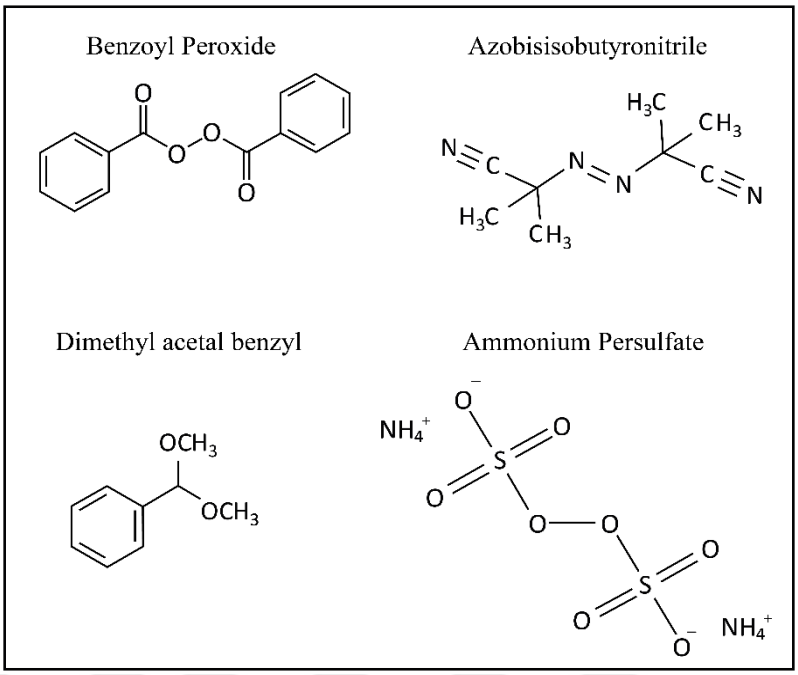

Figure 2.9. Certain initiators widely used in molecular imprinting applications.

2.4.3.5. Solvent / Porogen

In MIP synthesis, it acts as both a pore builder and a solvent for other components participating in the process. It significantly influences the interactions between the template-functional monomer, thereby affecting the the morphological structure of the polymer. The solvent quantity is a critical factor in polymer synthesis, akin to other components. Excessive solvent usage weakens the interactions between the functional monomer and the template molecule, leading to the formation of polymers with reduced binding capability. Additionally, the polarity of the solvents used influences the interactions between the template and the functional monomer. Solvents with low polarity facilitate the formation of pre-complexes, whereas those with high polarity negatively affect the interaction dynamics that support the assembly of the pre-complexes. Solvents such as distilled water, ethanol, acetone and chloroform are frequently employed in MIP synthesis to enhance the selective recognition of particular compounds (Ma et al., 2017; Włoch and Datta, 2019).

2.5. Polymerization Types Used for MIP Synthesis

2.5.1. Bulk Polymerization

With this method, a solid polymer is obtained as a result of the polymerization process using the basic components required for MIP synthesis. The method is straightforward to implement, resulting in rapid polymer synthesis. The synthesized polymer is subjected to laborious and time-consuming physical processes such as sieving, grinding or crushing. As a result of these processes, particles with irregular shapes and unequal sizes are obtained. However, uniform size and regular shape are very important issues for various applications and areas where MIPs are used. Additionally, these physical processes lead to some loss of polymer material. Since it is an exothermic process, the scale-up process in this polymerization causes high heating of the sample. In addition, it has been determined that the polymers synthesized using this method have poor reusability and selectivity properties (Yan and Row, 2006; Włoch and Datta, 2019; Arabi et al., 2021).

2.5.2. Precipitation Polymerization

It is a method in which polymers with regular shapes and sizes can be synthesized with high efficiency. In order to prevent the components to be used from coming together and forming clusters, polymerization is performed in dilute solution and the polymers are precipitated into spherical particles. Compared to bulk polymerization, a lot of solvent is needed. Particle sizes of synthesized polymers are affected by polymerization conditions such as temperature, type of solution used, and mixing speed (Yan and Row, 2006; Włoch and Datta, 2019; Arabi et al., 2021).

2.5.3. Suspension Polymerization

Suspending agents and high mixing speed are used to avoid the formation of monomeric clusters and to ensure the dispersion of monomers in an aqueous phase in the form of droplets. With this polymerization method, monomer droplets are combined to form regular structures. Depending on the polymerization conditions used, droplets of varying sizes (µm-mm) can be produced (Vivaldo-Lima et al., 1997; Bijhanmanesh and Etesami, 2016). There are two distinct methods of suspension polymerization. The polymer formed in the first of these can be dissolved in its monomer. In this way, properly shaped polymeric particles are obtained and based on the shape of the particles formed, it is referred “bead polymerization”.

In the other case, the polymer cannot be dissolved in its monomer and irregularly shaped particles are obtained. This is known “powder polymerization” (Kotoulas and Kiparissides, 2006) Suspension polymerization is preferred for large-scale applications (Włoch and Datta, 2019).

2.5.4. Emulsion Polymerization

Emulsion polymerization is a polymerization method that is broadly employed in the production of various polymers and offers various advantages over other polymerization methods. This method is based on dispersing monomer droplets in an aqueous phase containing an emulsifier to stabilize the droplets and prevent coalescence. It is an attractive technology that offers the opportunity to control particle distribution and dimension in the preparation of polymers and polymer composites. The polymerization process can be optimized by adjusting parameters like emulsifier amount, monomer type, and reaction conditions, thereby tailoring the properties of the resulting polymers (Asua, 2004 ; Zhang et al., 2013).

2.6. Nanotechnology

The term nanoscience is attributed to Richard Feynman, who in 1959 gave a forward-looking talk titled “There’s Plenty of Room at the Bottom.” In this speech, Feynman introduced the idea that atoms could be manipulated individually, laying the groundwork for nanotechnology. He stated that the principles of physics do not oppose the possibility of maneuvering things atom by atom, thereby offering a new perspective to the fields of science and engineering. Feynman's visionary ideas have since become foundational to the advancements in nanotechnology research (Schaming and Remita, 2015). Norio Taniguchi first introduced the term "nanotechnology" in 1974, and the term covers the adjustment of materials at the nano-scale (such as processing, separation, consolidation and deformation at the atomic or molecular level) (Zietek et al., 2021; Verma et al., 2018; Katas et al., 2018; Lawal et al., 2022; Raj et al., 2023; Gitea et al., 2020; Wang et al., 2022; Garip et al., 2022). After the term nanotechnology began to be spoken in the scientific world, significant developments have been experienced in the imaging and characterization of nano-sized objects. Scanning Tunneling Microscopy (STM) and Atomic Force Microscopy (AFM) devices, invented in the 1980s, have revolutionized the field of nanotechnology by allowing

imaging, characterization and manipulation of materials at the atomic and nano-scale. These devices have enabled researchers to examine the surface structures of materials at the atomic level and have contributed greatly to the rapid advancement of nanotechnology (Binnig and Rohrer, 1987; Binnig et al., 1986; Ondráček et al., 2011; Kurra and Reifenberger, 2014).

Initiated by Taniguchi, continuing with the discovery of fullerenes in the 1980s and Eric Drexler's proposal of nanoscale assemblers in the 1990s, nanotechnology has undergone a significant evolution over the years, with notable advances occurring in various sectors. (Hulla et al., 2015). Nanotechnology has found wide use in many fields, including health, materials science, energy, textile and food industry studies (Sun and Gupta, 2019; Mohamed, 2017).

Nanotechnology has facilitated the advancement of targeted drug delivery systems by enabling the creation of specific smart drug carriers for therapeutic purposes. In addition, nanotechnology has been effective in applications such as regenerative medicine, plastic surgery and cancer treatment and has contributed to the advancement of healthcare services (Tan et al., 2016). Moreover, the integration of nanotechnology in dentistry has opened new possibilities to improve oral health through innovative materials and treatments (Verma et al., 2018).

It has pioneered the advancement of new composite materials that reveal the versatility and potential of nanomaterials in materials science (Zietek et al., 2021). The integration of nanotechnology with different disciplines has enabled the production of a wide variety of nanoscale functional materials. Solar cells, designed for sustainability purposes especially in the fields of environment and energy, are an important example of nanotechnology (Wang et al., 2022). Likewise, lightweight and durable nanotechnology materials have begun to increase in the textile industry and construction sectors (Saleem and Zaidi, 2020).

Nanotechnology has made a decisive contribution to the transformation of the food sector, with many applications aimed at improving food safety and quality. Integrating nanoparticles into food products and packaging has made great progress in the industry by improving various aspects of food processing and preservation processes (Shafiq et al., 2020).

Nanomaterials have been effective in improving packaging properties, particularly in areas such as flexibility and gas barrier, allowing food products to stay fresher for longer (Sharma et al., 2017).

2.7. Nanomaterials

Nanostructured materials serve as a materials characterized by their nanoscale dimensions, consisting of grains, particles, fibers or other components. They are classified into four distinct categories depending on their dimensions from zero to three (0D-3D). These materials possess distinctive physical and chemical traits attributed to their dimensions, morphology, and surface features. With their large surface area relative to volume, advanced reactivity, and quantum phenomena, they possess functionalities not observed in other materials. Nanomaterials include physical properties such as optical, magnetic, mechanical and catalytic, as well as chemical properties such as surface reactivity, stability and functionalizability (Webster et al., 2005). The usage areas of nanomaterials are quite wide and they find application in various fields.

For example, thanks to their high efficiency and improved performance, they can be used in energy technologies such as solar cells (Saleem and Zaidi, 2020). They are also used in medicine to deliver targeted and personalized treatment options in fields including biomedical imaging, therapeutic delivery, and tissue engineering (Webster et al., 2004). Nanomaterials also play important roles in environmental improvement, with applications including water treatment, air cleaning, and removal of pollutants. In addition, nanomaterials contribute to sustainable agricultural practices by using them for crop protection, nutrient distribution and soil improvement in the agricultural field (Saleem and Zaidi, 2020).

The strengths of nanomaterials lie in their distinctive properties, enabling enhanced performance and innovative functionalities across various applications. Nanomaterials exhibit improved reactivity, selectivity, and efficiency compared to conventional materials, rendering them invaluable in catalysis, sensing, and drug delivery (Wohlleben et al., 2017). Their ample surface area fosters heightened interactions with target molecules, leading to enhanced sensitivity and specificity in biosensing applications (Zhang et al., 2022). Moreover, the adjustable properties of nanomaterials, comprising shape, dimension, and surface chemistry,

offer customization options to meet specific requirements in diverse industries, driving innovation and tailored solutions (Bleeker et al., 2013). The adaptability and versatility of nanomaterials render them indispensable in advancing technologies and tackling intricate challenges across various sectors.

2.8. Nanoparticles and Its Production Techniques

Nanoparticles are defined as particles characterized by distinct features including a high surface/volume ratio, stability, robustness, functional versatility, and optical activity. They can be derived from a diverse range of organic and inorganic materials, including carbon, polymers, ceramics, and metals, and are categorized as organic, inorganic, or carbon-based nanoparticles based on their constituent material (Ealia and Saravanakumar, 2017). Nanoparticles' dimension and shape exert a critical influence on their properties (Yuan et al., 2012).

Nanoparticles essentially consist of three distinct layers, classified as the surface, shell, and core. The surface is the outermost layer of the nanoparticle and can be functionalized using a wide variety of molecules. The shell is an intermediate layer located between the surface and the core, enveloping the core and aiding in its protection. Finally, the core is the primary component that constitutes the nanoparticle and is situated at the center (Shin et al., 2016).

Nanoparticles have a wide potential for use in various fields due to their unique properties. Nanoparticles have been successfully used in a diverse array of applications, from catalytic applications to electronics and biology, to materials science, highlighting their versatility in interdisciplinary fields (Virkutytė and Varma, 2011). Additionally, it is stated that nanoparticles are promising in sensor applications, materials engineering, biomedical applications, regenerative medicine, energy management, and environmental technology (Zhang et al., 2019).

Nanoparticles are indispensable in delivering pharmaceuticals, diagnosing illnesses, and providing effective therapies. They are used as alternative antimicrobial agents to combat antibiotic resistance and detect pathogenic bacteria, as well as operate as delivery vehicles for emerging pharmaceuticals and vaccines (Bai et al., 2018). Nanoparticles, especially those

derived from precious metals such as silver and gold, are indispensable in medical applications due to their high biocompatibility, stable structure and large-scale production possibilities (Klębowski et al., 2018).

Nanoparticles are synthesized through primary synthesis approaches, known as top-down and bottom-up methods, which encompass a variety of sub-synthesis techniques (Ealia and Saravanakumar, 2017).

The “top-down” method entails the synthesis of nanoscale materials by fragmenting larger materials. This technique is frequently executed using lithographic methods or chemical processes. For instance, in the synthesis of nanoscale materials, this approach is preferred for creating nanostructures by fragmenting larger materials (Yu et al., 2013).

The “bottom-up” method involves constructing nanoscale materials from fundamental building blocks. This method enables the assembly of small particles into nanostructures. This technique offers precise control in the creation of nanostructures and the flexibility to be utilized in various applications (Gour and Jain, 2019).

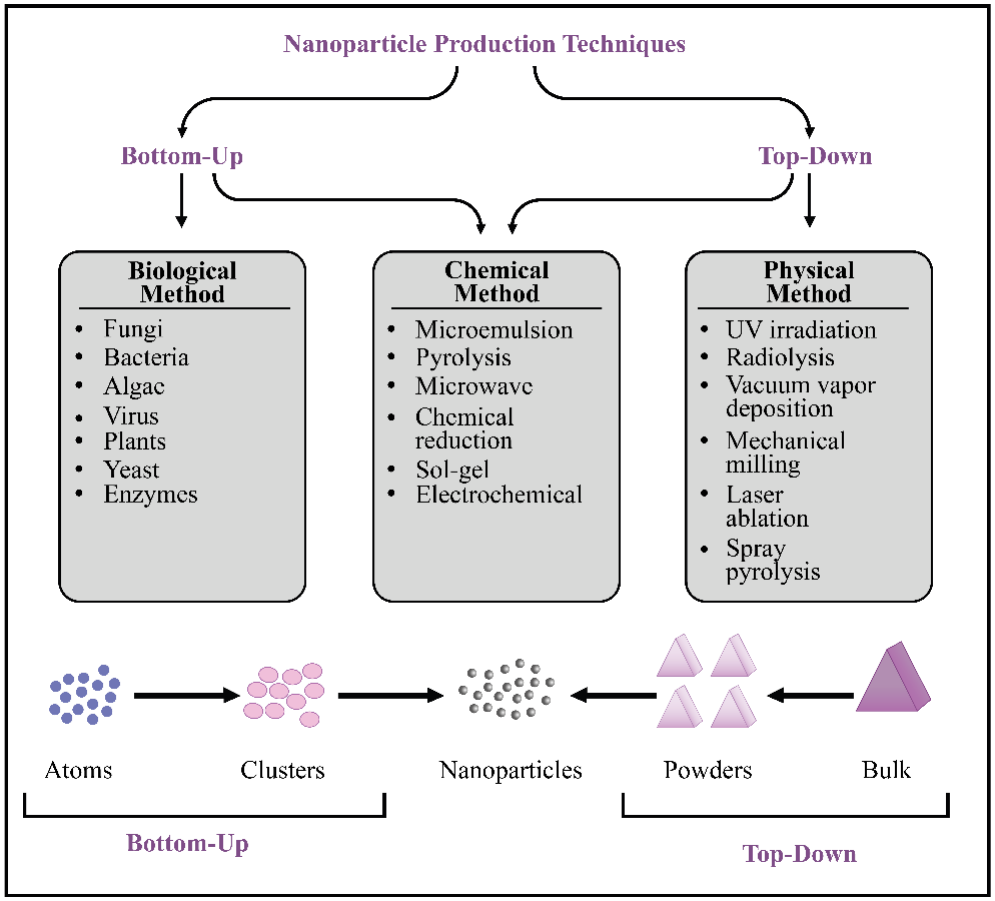

Figure 2.10. Diagram of various production techniques of nanoparticles.

3. MATERIALS AND METHOD

3.1.Materials

AgII, polyvinyl alcohol (PVA), sodium dodecyl sulfate (SDS), sodium bicarbonate, 1-vinyl imidazole (VIM), 2-hydroxyethyl methacrylate (HEMA), ethylene glycol dimethacrylate (EGDMA), sodium bisulfite and ammonium persulfate (APS) were obtained from Sigma (St. Louis, MO, USA). Ethanol used in washing processes and phosphate buffered saline (PBS) and sodium chloride (NaCl) used in desorption studies were also purchased from Sigma. All chemicals taken are of analytical purity and were stored under appropriate storage conditions until used in experimental studies.

3.2. Preparation of Nanoparticles

AgII served as the template molecule for nanoparticle synthesis. Polymerization executed in a polymerization reactor (Radleys Carousel 6 Plus Reaction Station, UK) at 40°C for 24 hours using a mixture of first liquid phase (aqueous solution of PVA (100 mg), SDS (15 mg) and sodium bicarbonate (12.5 mg)(5 mL)), second liquid phase (aqueous solution of PVA (50 mg) and SDS (50 mg)(100 mL)), monomer phase (AgII:VIM (0.1 mL), HEMA (0.25 mL), EGDMA (1 mL)), sodium bisulfite (50 mg) and APS (75 mg). First, the prepared monomer phase was added to the first liquid phase. The mixture suffered homogenization in a homogenizer at 30.000 rpm for 30 minutes to generate a miniemulsion. In the meantime, AgII-VIM pre-complexes were prepared separately by mixing AgII and VIM in different molar ratios (1:1, 1:5, 1:10, and 1:20) and kept at +4°C for a duration of 4 hours. At the end of this period, each pre-complex sample was analyzed spectrophotometrically. The most effective AgII-VIM pre-complex determined was added to the mixture and the mixture was stirred for an additional 10 minutes. The miniemulsion containing the AgII-VIM pre-complex was subsequently added gradually to the second liquid phase. The entire mixture was transferred to the polymerization reactor, which was then heated to 40°C and stirred at 400 rpm. Ultimately, sodium bisulfite and APS were introduced, initiating a 24-hour polymerization process. The synthesized nanoparticles were rinsed with 20 mL of distilled water and afterward with 20 mL of ethanol to eliminate chemicals and impurities not involved in the polymer structure. Following each washing step, the solution containing nanoparticles underwent centrifugation (Allegra X-30r Centrifuge, Beckman Coulter, Germany) at 25.000

rpm for 40 minutes. Finally, the nanoparticles were treated for 2 hours with a desorption solution of PBS (5 mL) (10 mM, pH 7.4) containing 0.03 M NaCl to remove AgII. Then the solution was centrifuged again at 25.000 rpm for 40 minutes. At the conclusion of all procedures, the supernatant was collected, and absorbance measurements were acquired spectrophotometrically (at a wavelength of 200 nm). The process was iterated until there was no remaining AgII within the polymeric structure. Removing the template revealed certain cavities for AgII. In this way, it was understood that there would be no problems in removing the template molecule from the structure in the later stages of the study. The same procedure was used to form NIP polymers devoid of AgII molecules.

Figure 3.1. Polymerization reactor and high-speed centrifuge used for AgII-MIP and NIP nanoparticle synthesis.

3.3. Characterization of Synthesized Nanoparticles

For characterization purposes, the nanoparticles underwent analysis through Zeta-size analysis, Transmission Electron Microscopy (TEM), Scanning Electron Microscopy (SEM), and Fourier-Transform Infrared Spectroscopy (FTIR). The nanoparticle dimensions and their distributions were evaluated through Zeta-size analysis, while their surface morphologies and

particle sizes were examined using SEM and TEM, and their chemical structures were assessed via FTIR.

3.3.1. Zeta-size Analysis

A Zeta-sizer is a device that provides the ability to measure properties of particles or molecules in liquid media, such as particle size, zeta potential and molecular weight. It works with the dynamic light scattering method with its detector located at a 90-degree angle and measures particle size with this method. Particle sizes of AgII-MIP and NIP nanoparticles were determined using the Zetasizer Nano S-90 (Malvern Instruments, London, UK). For this purpose, nanoparticle samples dissolved in distilled water were placed in the sample compartment of the device (approximately 1 mL) and measurements were taken at least three times at room temperature.

3.3.2. Transmission Electron Microscopy Analysis

Size and structural analysis of nanoparticles was conducted utilizing a transmission electron microscope (TEM) (Hitachi HT7700, Tokyo, Japan). Nanoparticles were dissolved in ethanol and dispersed into the solution. Subsequently, it was placed on a carbon film-covered copper grid and left to dry at room temperature. Images of the dried nanoparticle samples were taken at different zoom levels.

3.3.3. Scanning Electron Microscopy Analysis

A scanning electron microscope (SEM) (FEI, Quanta 650 Field Emission, USA) was employed to scrutinize the surface morphologies and particle dimensions of both AgII-MIP and NIP nanoparticles. First, the nanoparticles were ensured to be thoroughly dispersed in ethanol. A sonicator (Wuc-A06h, Daihan Scientific, Korea) was used to disperse nanoparticles effectively. Nanoparticle samples prepared with ethanol were dried using an oven (Mlf 120, Mikrolab, Turkey). The dried nanoparticle samples were placed on the sample plate with the help of conductive adhesive, and the surface of the samples was gold coated in a vacuum environment to obtain clearer images. Thereafter, the nanoparticle samples were visualized under varying magnifications.

3.3.4. Fourier Transform Infrared Spectroscopy Analysis

Chemical structure analysis is important in determining whether nanoparticles are synthesized correctly. For this purpose, the chemical structure of the synthesized AgII-MIP and NIP nanoparticles was examined by fourier transform infrared spectroscopy (FTIR) (Jasco, FT/IR-6700, USA). Nanoparticle samples were used in analysis in solid (powder) form. The samples were scanned across the wave number range of 400-4000 cm^{-1}, and spectra were registered.

3.4. Modification of SPR Chip Surface with Allyl Mercaptan

The gold surface of the SPR chip to be used was modified with allyl mercaptan solution before being coated with nanoparticles. First, the chip was subjected to acidic piranha solution (15 mL) prepared with 30% hydrogen peroxide (H_2O_2), 30% ammonia (NH_4OH), and distilled water for a period of time. Following this process, the chip was washed using ethanol and distilled water. The cleaned chip was placed in the oven and dried (It has 200 mmHg vacuum, 40°C, approximately 1 h) . When the drying process was completed, 20 µl of allyl mercaptan was deposited onto the chips' surface and left overnight. At the end of this period, the chip was washed again, and dried. With this process, a chip surface with thiol (–SH) groups that are expected to interact with polymers was created **(Figure 3.2.).**

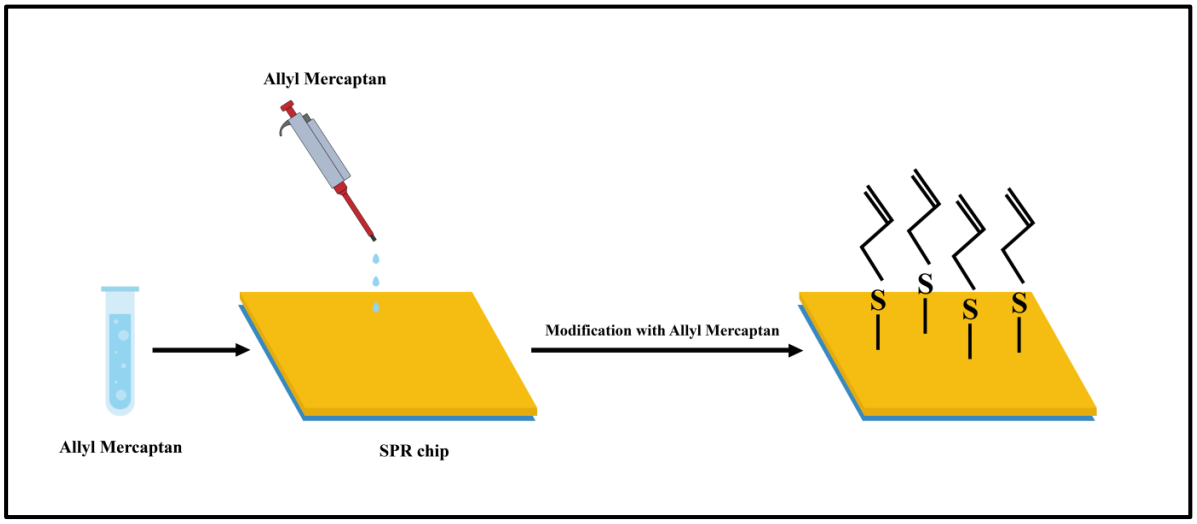

Figure 3.2. Allyl modification.

3.5. Preparation of AgII-MIP and NIP Nanoparticle-based SPR Chips

Before the nanoparticles were adhered to the surface of the SPR chip, the gold surface of the chip was cleaned with acidic piranha solution and then modified with allyl mercaptan. Then, AgII-MIP nanoparticles (20 μL solution) were dropped onto the chip surface and spread on the chip surface using the spin coating technique. The chip was exposed to a UV lamp (365 nm, 100 W) (Analytik Jena, Jena, Germany) for a duration of 30 minutes. Thereby, the AgII-MIP nanoparticles coated on the chip surface were ensured to adhere to the surface. After surface coating, the SPR chip surface was washed with distilled water and ethanol. Lastly, the chip was dried in a vacuum oven at 40°C under a pressure of 200 mmHg. The identical procedures were repeated utilizing NIP nanoparticles, resulting in the fabrication of a control chip. The abbreviations AgII-MICspr are used for the SPR chip coated with AgII-MIP nanoparticles, and NICspr are used for the SPR chip coated with NIP nanoparticles.

3.6. Characterization of SPR Chips

Surface characterization of SPR chips was carried out by atomic force microscopy (AFM) (Park Systems AFM, Park NX10, South Korea) and contact angle (Attension Theta Lite, Biolin Scientific Ltd., Sweden). Contact angle measurements were conducted to illustrate the presence of AgII-MIP and NIP nanoparticles on the SPR chip surface and to assess the surface hydrophilic-hydrophobic properties. In addition, atomic force microscope images were taken to demonstrate the presence of nanoparticles on the chip surface, to determine the surface depths of AgII-MICspr and NICspr chips, and to show whether the nanoparticles were distributed homogeneously on the chip surface.

3.6.1. Atomic Force Microscopy Analysis

Atomic force microscopy (AFM) is a three-dimensional imaging with high atomic resolution used for surface characterization. It is a type of scanning probe microscope and the imaging process is performed depending on the interaction between a sharp tip (lever) and the atoms of the surface (Vahabi et al., 2013). Surface characterization of AgII-MICspr and NICspr chips was examined using AFM (Park Systems AFM, Park NX10, South Korea). Cspr (non-coated SPR chip), AgII-MICspr and NICspr chips were fastened to the sample holder with the help of a adhesive tape and imaging was executed. The surface depths of the Cspr, AgII-MICspr, and NICspr chips were determined.

3.6.2. Contact Angle

Cspr, AgII-MICspr and NICspr were utilized to evaluate the hydrophobic/hydrophilic properties of SPR chip surfaces. The contact angle values of Cspr, AgII-MICspr and NICspr chips were determined with the Attension Theta Lite (Biolin Scientific Ltd., Sweden) brand device by dropping a drop of water on the chip surface. Many measurements were taken from two different positions of the chip and the contact angles were computed by averaging these measurements.

3.7. Kinetic Analysis Studies using AgII-MICspr Sensor Chip

After the preparation of AgII-MICspr chip, binding and kinetic studies were performed with AgII solutions at different concentrations. The studies were carried out using the Bionavis brand Otso model SPR device (Spr Navitm 200 Otso, Bionavis, Finland). First, the nanoparticle-coated surface of the AgII-MICspr chip was placed in the sample holder in the device with the flow cell direction. Then, the system was balanced by passing 10 mM PBS (pH: 7.4) (30 µL/min flow rate) through the system. While the buffer solution was passing through the system, surface plasmon curves were taken and the resonance angle was determined. After equilibration, pH: 7.4 PBS containing 0.03 M NaCl was passed through the system (30 µL/min flow rate) and AgII molecules were extracted from the AgII-MICspr chip surface. Thus, specialized cavities for AgII were created on the nanoparticles located on the chip's surface. The amount of AgII removed was determined by the ΔR value from the sensorgram. The system was balanced again, and after this balancing step, AgII solutions prepared in 10 mM PBS (pH: 7.4) at concentrations ranging from 3 pg/mL to 100 pg/mL were passed through the system (15 µL/min flow rate), the system was waited to reach equilibrium, and the response (ΔR) of the sensor was examined. Afterwards, the desorption process was carried out by passing desorption solution (0.03 M NaCl + 10 mM, pH: 7.4 PBS) through the system. After the desorption process, the system was regenerated by washing with PBS (10 mM, pH: 7.4) for 10 minutes. Then, sensorgrams were obtained using device software. ΔR values were determined from the sensorgrams of each concentration value. A calibration chart was created based on these data. Studies were repeated at least three times and mean values were used in the analysis and standard deviations were calculated.

3.8. AgII Competitive Binding Kinetic Analyzes using SPR Chips

In order to demonstrate the AgII selectivity of the SPR sensor fitted with AgII-MICspr/NICspr chips, AgI and vasopressin (Vp) were introduced to evaluate selectivity as competing compounds (Ertürk et al., 2016; Esentürk Koca et al., 2019; Erdem et al., 2019). AgII, AgI, and Vp solutions prepared at 15 pg/mL concentrations in 10 mM PBS (pH: 7.4) were sent to the SPR sensor (15 µL/min, for 30 min) and sensorgrams were taken. After each measurement, a desorption process was applied to remove the substances adsorbed on the surface. The same operations were performed with the SPR sensor fitted with the NICspr chip. The selectivity and imprinting selectivity coefficients of the chips were calculated using the following formulas:

The selectivity coefficient was calculated using the equation $k = \Delta R_{template} / \Delta R_{competitor}$, while the imprinting selectivity coefficient was calculated using the equation $k' = k_{imprinted}/k_{control}$.

3.9. Reusability Studies

To assess the reusability and efficiency of AgII-MICspr chip, repeated measurements were conducted using AgII solutions at a concentration of 15 pg/mL. For this purpose, AgII solutions were given 10 consecutive times (with a flow rate of 15 µL/min) to the SPR sensor system to which AgII-MICspr chip was installed and their sensorgrams were taken.

3.10. AgII Detection from Human Serum Samples

Analyzes were performed using a human serum sample obtained from Sigma-Aldrich (St. Louis, USA). First, the serum sample was placed in tubes containing ethylenediaminetetraacetic acid (EDTA) to separate serum and cells and was centrifuged (3800 rpm, 30 min). The supernatant taken after centrifugation was filtered and stored at -20 ˚C to be used in analyses. The serum sample in which AgII was not determined was used as a blank sample. AgII was added to this sample externally at varying concentrations (3, 15, 50 and 100 pg/mL). The serum was mixed with 10 mM PBS (pH 7.4) in a 1:10 proportion to achieve dilution. The diluted samples were passed through the SPR sensor and ΔR changes were examined.

4. ANALYSIS AND DISCUSSIONS

4.1. Pre-complex Preparation and Nanoparticle Synthesis

In order to determine the molar ratio in which AgII and VIM molecules form the most effective pre-complex, AgII-VIM mixtures were formulated in mole ratios of 1:1, 1:5, 1:10 and 1:20 (n_{AgII}:n_{VIM}). Mixtures incubated at +4°C for 4 hours. Then, these pre-complex mixtures were compared with UV spectrophotometer (Genesys 150, Thermo Scientific, USA) and the most suitable molar ratio was found to be 1:10 (n_{AgII}:n_{VIM}). AgII-MIP and NIP nanoparticles were synthesized by the method given in section 2.2 by using the pre-complex in this determined molar ratio. The nanoparticles obtained at the end of the polymerization were washed with distilled water and ethanol to remove the chemicals that did not participate in the polymerization reaction. After washing, a desorption solution of PBS (10 mM, pH 7.4) containing 0.03 M NaCl was used to remove the template molecule from the polymeric structure. AgII removed from the structure during desorption processes was determined by absorbance measurements at 200 nm wavelength with a UV spectrophotometer. According to absorbance measurements, it was observed that 92% of AgII was removed from the polymeric structure at the end of desorption. Thus, it was observed that the applied desorption solution effectively released the template molecule from the nanoparticle structure. Consequently, it was determined that this solution could be used efficiently to release AgII from nanoparticles to be coated on the SPR chip surface.

4.2. Nanoparticle Characterization

4.2.1. Zeta-size Analysis

Zetasizer Nano-S90 device (Malvern Panalytical, England) was used to determine the sizes of AgII-MIP and NIP nanoparticles. All measurements were independently repeated in triplicate and the averages were taken. The findings indicated that the sizes of AgII-MIP and NIP nanoparticles were 46.51 nm and 48.97 nm, respectively (**Figure 4.1.**).

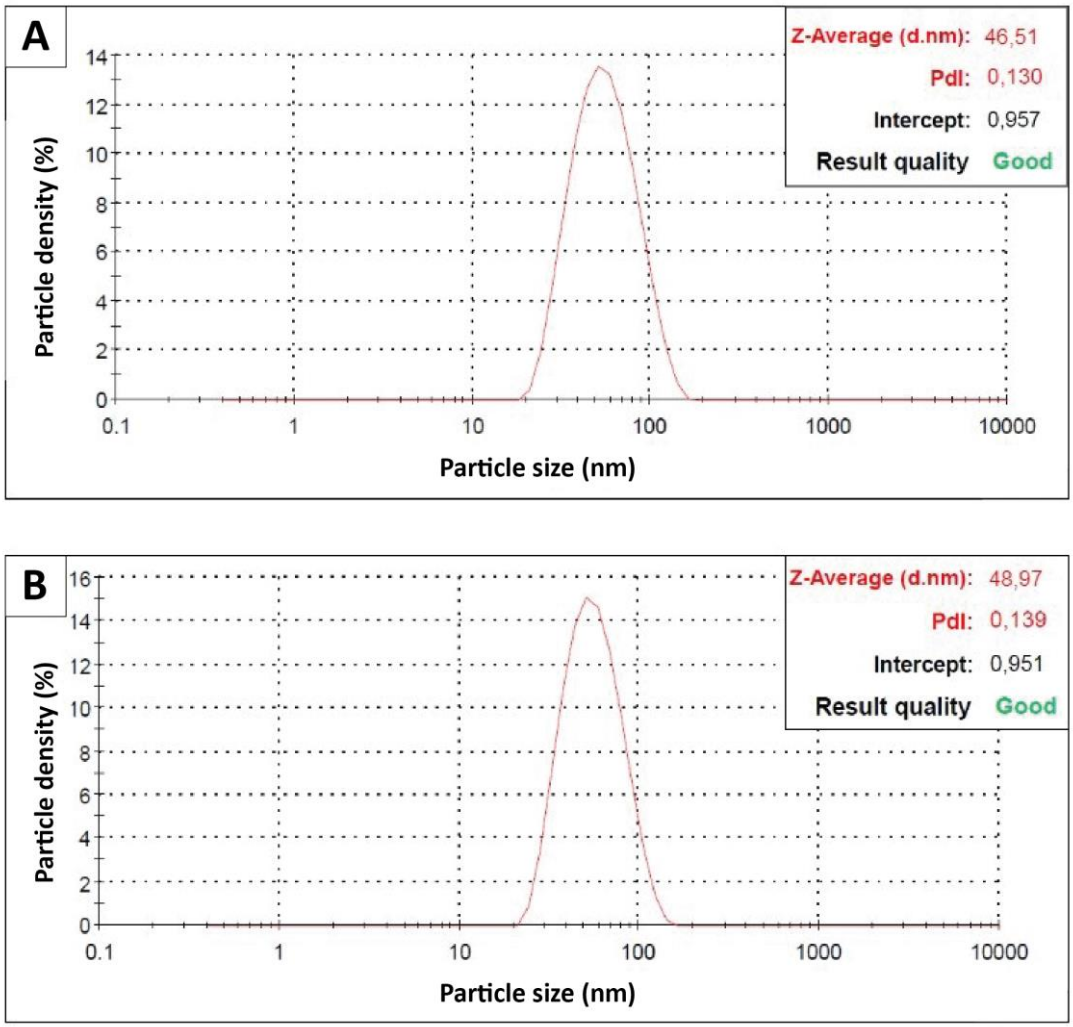

Figure 4.1. Zeta-size analysis of nanoparticles A) AgII-MIP, B) NIP.

4.2.2. Transmission Electron Microscopy Analysis

The sizes and morphological structures of the nanoparticles were investigated by TEM using different zoom ratios (100x for AgII-MIP, 120x for NIP). The findings showed that the particles were smaller than 50 nm in size, had a rough surface and a round-shaped (**Figure 4.2.**).

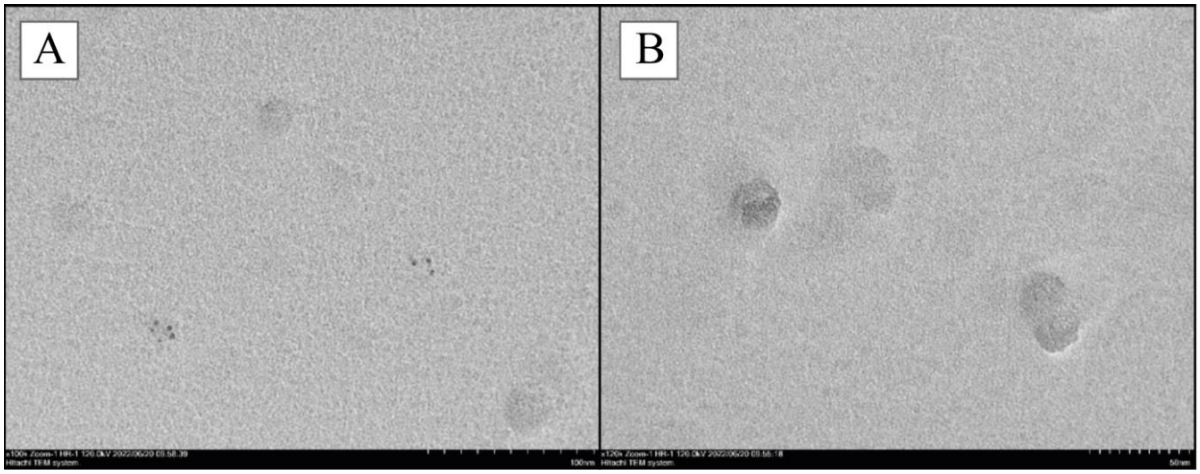

Figure 4.2. TEM images of nanoparticles, A) AgII-MIP (100x), B) NIP (120x).

4.2.3. Scanning Electron Microscopy Analysis

The surface morphologies and particle dimensions of AgII-MIP and NIP nanoparticles were assessed using a SEM device from FEI, Quanta 650 Field Emission, at varied magnifications (600.000x and 400.000x). The findings are presented in **Figure 4.3**. The particle sizes of AgII-MIP and NIP nanoparticles were identified to be within the range of 20-40 nm. It was noted that the particle size distribution exhibited homogeneity. The outcomes obtained through these three methods align well with each other.

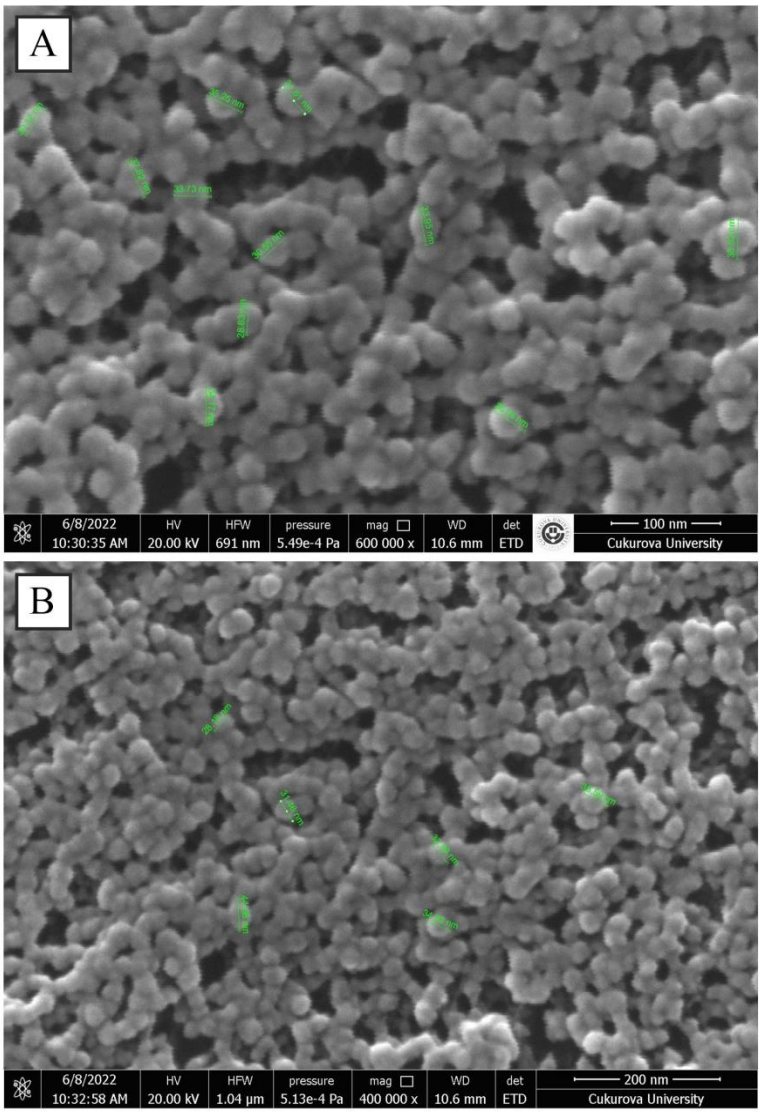

Figure 4.3. SEM images of A) AgII-MIP nanoparticles (600.000x), B) NIP nanoparticles (400.000x).

4.2.4. Fourier Transform Infrared Spectroscopy Analysis

The chemical compositions of AgII-MIP and NIP nanoparticles were ascertained through Fourier transform infrared spectroscopy (FTIR). The spectra of FTIR analyzes of nanoparticles are depicted in **Figure 4.4**.

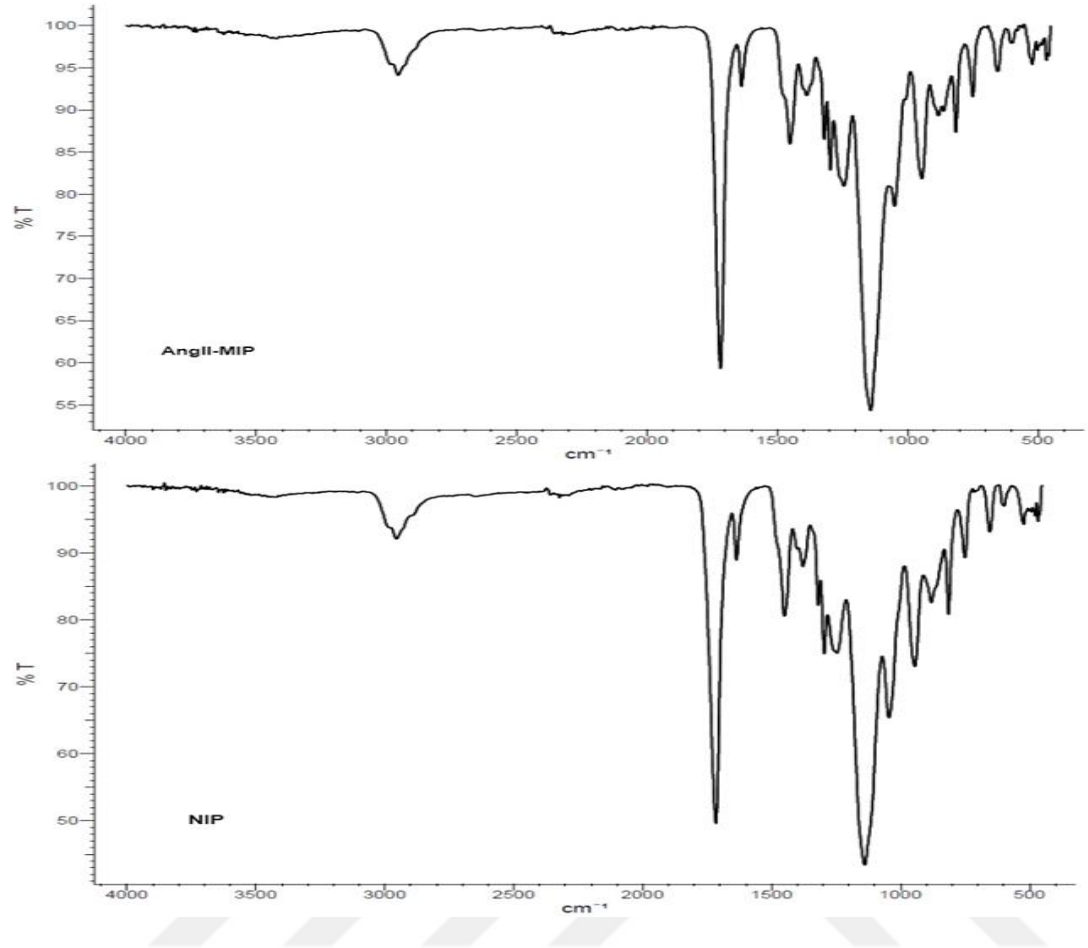

Figure 4.4. FTIR spectra of A) AgII-MIP and B) NIP nanoparticles.

Since the chemical structures of AgII-MIP and NIPs are resemble, their FTIR spectra are also similar. The peak observed around 3327 cm^{-1}, which belongs to the O-H band (stretching), is common to both nanoparticles. This peak arises from HEMA present in the structure of both nanoparticles. The C-H bands (stretching) seen near 2952 cm^{-1} correspond to HEMA and EGDMA structures, C=O bands (stretching) seen around 1718 cm^{-1} belonging to the carbonyl group found in the structure of EGDMA, and C-O bands (stretching) seen near 1138 cm^{-1} are common in AgII-MIP and NIP nanoparticles. The 1220-1200 cm^{-1} peaks seen in AgII-MIP are bands belonging to amine groups. The peak around 1637 cm^{-1} seen in AgII-MIP indicates the presence of C=C and C=N bands (vibration). These bands are attributed to the AgII-VIM in AgII-MIP. It is observed that the intensity of the C–O bands around 1246 cm^{-1} in AgII-MIP is higher compared to NIP. The presence of this peak originates from the VIM molecule and shows that VIM participates in the AgII-MIP structure. In addition, the presence of the band belonging to the carboxyl group at 1138 cm^{-1} in AgII-MIP also proves that the VIM molecule in the structure of the precomplex is included in the structure.

4.3. Preparation of AgII-MIP and NIP Nanoparticle-based SPR Chips

AgII-MIP and NIP nanoparticles were coated on the SPR chip surface with a spin coater. The nanoparticle-coated chips (AgII-MICspr and NICspr) were left under a UV lamp for 30 minutes, so ensuring that the nanoparticles adhered to the SPR chip surface (**Figure 4.5.**).

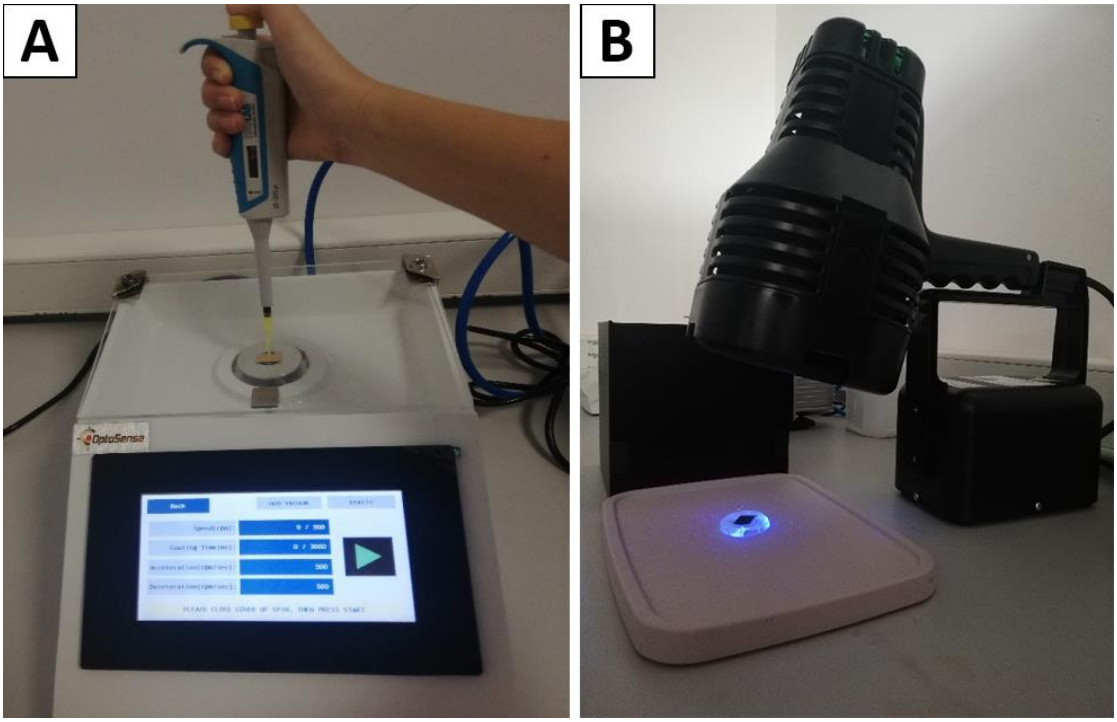

Figure 4.5. A) Coating the SPR chip surface with nanoparticles using spin coater and B) UV polymerization of SPR chip surfaces.

Figure 4.6. AgII-MICspr chip and NICspr chip.

After the nanoparticles were attached to the surface of the chips, washing processes were carried out. SEM analyzes (FEI, Quanta 650 Field Emission SEM, USA) were performed to check whether nanoparticles were released throughout the washing steps. Firstly, the chips were dried. The dried samples were fixed to the SEM sample plate. The surface of the fixed samples was made conductive by coating it with gold. Afterwards, SEM images of the samples were captured at various magnifications. When the SEM images of the SPR chips were examined, it was determined that the nanoparticles were distributed homogeneously on the chip surface and were held firmly on the chip surface (**Figure 4.7.**).

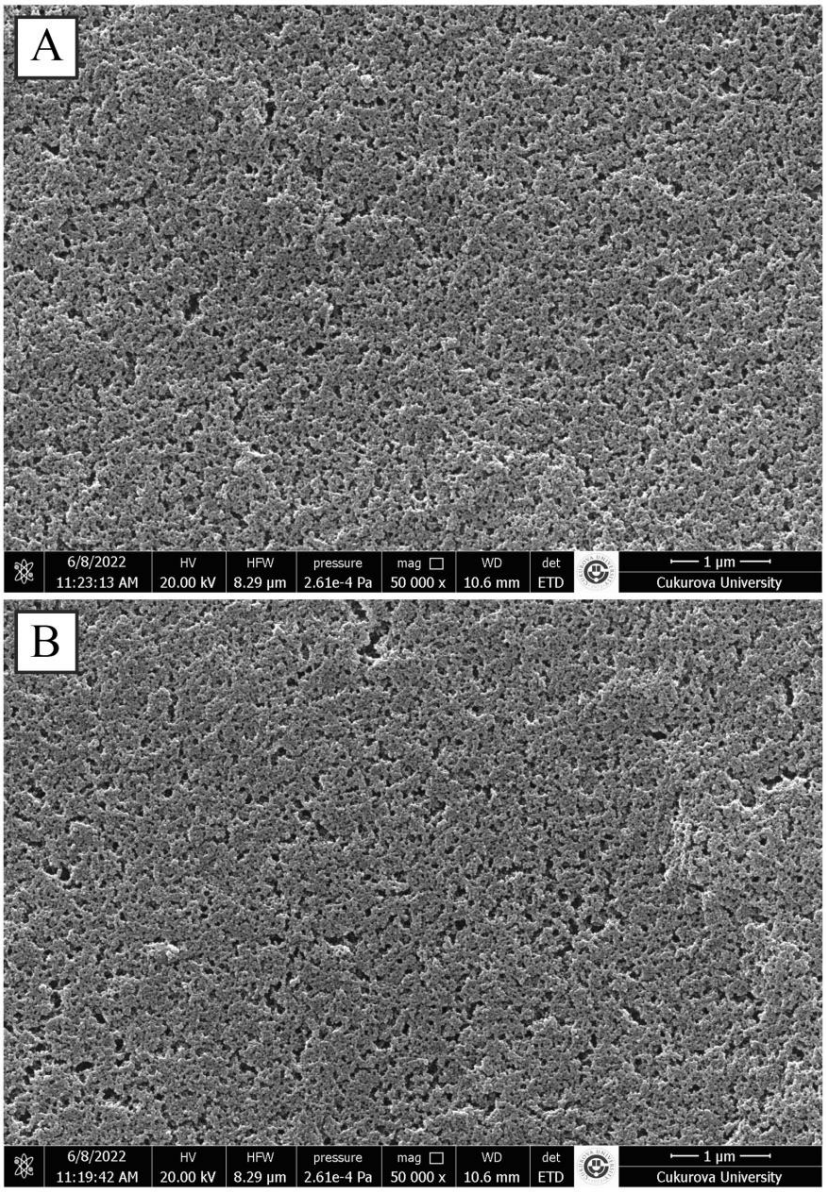

Figure 4.7. Surface images taken by SEM of A) AgII-MICspr chip (50.000x), B) NICspr chip (50.000x).

In addition, the prepared chips were placed in the SPR device (Spr Navitm 200 Otso, Bionavis, Finland) (**Figure 4.8.**) and it was tested whether stable sensorgrams could be obtained by passing distilled water at a flow rate of 30µL/min for both chips. As shown in **Figure 4.9.** and **Figure 4.10.**, a stable sensorgram was taken during the washing process for 30 minutes, and the absence of any fluctuation showed that the chip surface had a stable structure and the nanoparticles were held stably on the surface.

Figure 4.8. A) Placing the SPR chip into the device B) Taking sensorgrams from chips using an SPR device.

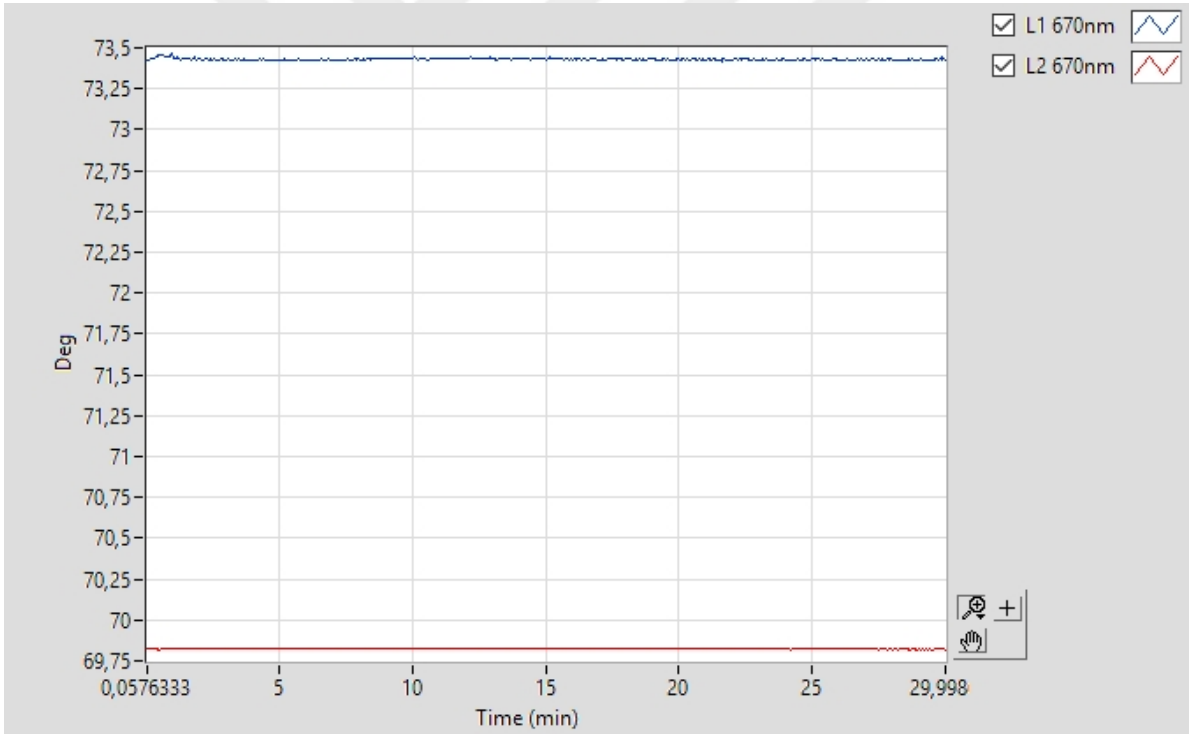

Figure 4.9. Sensorgram of AgII-MICspr chip.

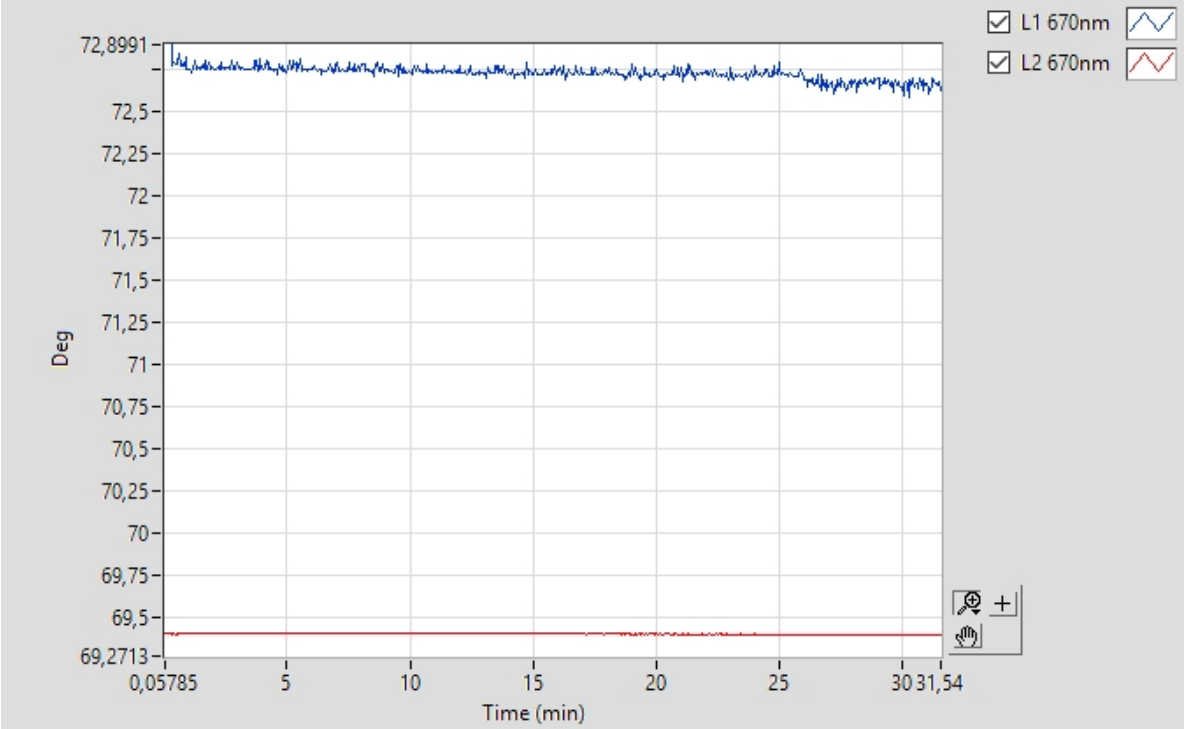

Figure 4.10. Sensorgram of NICspr chip.

4.4. Characterization of SPR Chips

4.4.1. Contact Angle

Contact angle measurements were made to determine the hydrophilic/hydrophobic characteritics of Cspr, AgII-MICspr and NICspr chip surfaces. A drop of water was dropped on different parts of the surface of each chip, and measurements were taken more than once from two points where the water drop touched the chip surface (right contact and left contact). With the contact angle values taken from these two contacting points, the average contact angle values, which are the average of both points, were obtained. The obtained contact angle values are given in **Figure 4.11**. Cspr, AgII-MICspr and NICspr chips's contact angle values were determined as 84°, 55.98° and 67.48°, respectively.

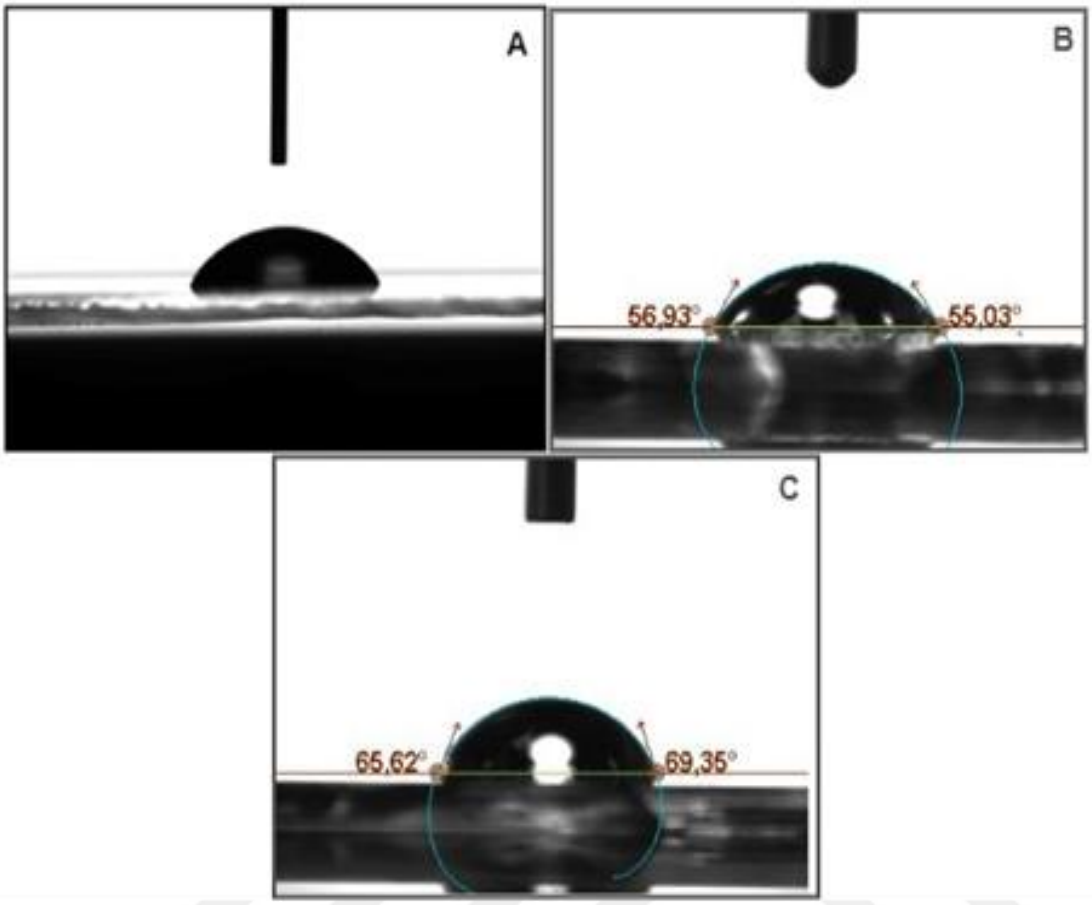

Figure 4.11. Contact angle measurements of A) Cspr chip, B) AgII-MICspr chip, and C) NICspr chip.

Upon assessing the results, it was ascertained that the contact angle value of the AgII-MICspr chip was lower than the contact angle value of the NICspr chip. The decline in the contact angle of the AgII-MICspr chip demonstrates that the chip surface is more hydrophilic. AgII-MICspr and NICspr chips were prepared using HEMA with hydrophilic characteristics. Functionalization of the chip surface with a hydrophilic layer promoted higher hydrophilicity. For this reason, it was observed that the contact angle values of AgII-MICspr and NICspr chips were lower than the Cspr chip. In addition, coating the chip surface with AgII-MIP and NIP caused roughness on the surface, which increased the wettability of the chip surface. It is thought that the reason why the contact angle of the AgII-MICspr chip is lower than the NICspr chip is due to the AgII and VIM molecules in the AgII-MICspr chip.

4.4.2. Atomic Force Microscopy Analysis

The surface morphologies and surface depths of Cspr, AgII-MICspr and NICspr chips were examined using AFM device in semi-contact mode. While the surface depth of the Cspr chip

was determined to be 5 nm, the surface depths of the AgII-MICspr and NICspr chips were found to be approximately 20–40 nm on average (**Figure 4.12.**). The findings show that the nanoparticles are distributed homogeneously on the chip surface.

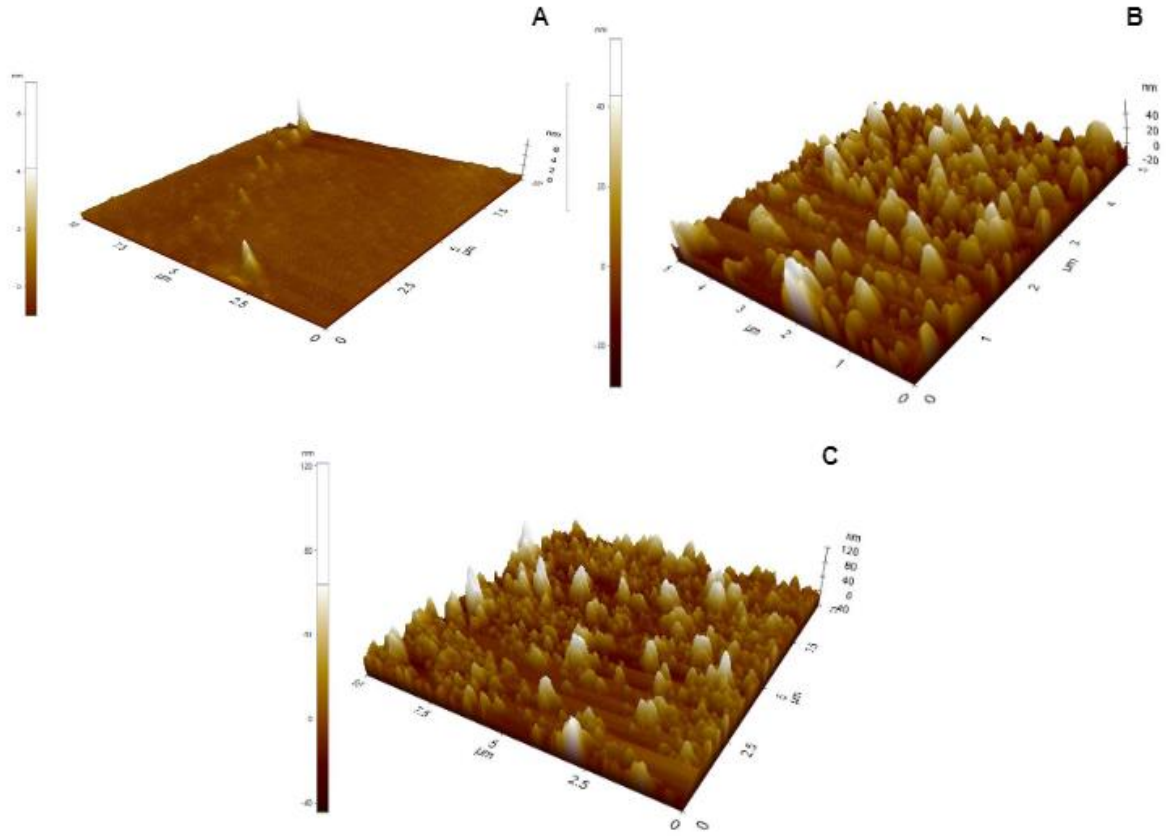

Figure 4.12. AFM images of A) Cspr chip, B) AgII-MICspr chip, and C) NICspr chip.

4.5. Kinetic Analysis Studies using AgII-MICspr Sensor Chip

The interaction characteristics and kinetic behavior of AgII in association with the AgII-MICspr chip were investigated. For this purpose, AgII solutions were prepared at different concentrations (3-100 pg/mL), and each AgII concentration prepared was interacted with the AgII-MICspr chip surfaces with the help of a peristaltic pump. Kinetic data were obtained using SPRview software. The variation in the signal over time, observed as the AgII molecule passes across the system, is shown in **Figure 4.13**. As the concentration of AgII increased, so did the SPR refractive index. The AgII-MICspr chip demonstrated sensitive detection capabilities, even for very low concentrations of AgII (3 pg/mL). These results validate the high affinity and selectivity in the interaction between the analyte and ligand.

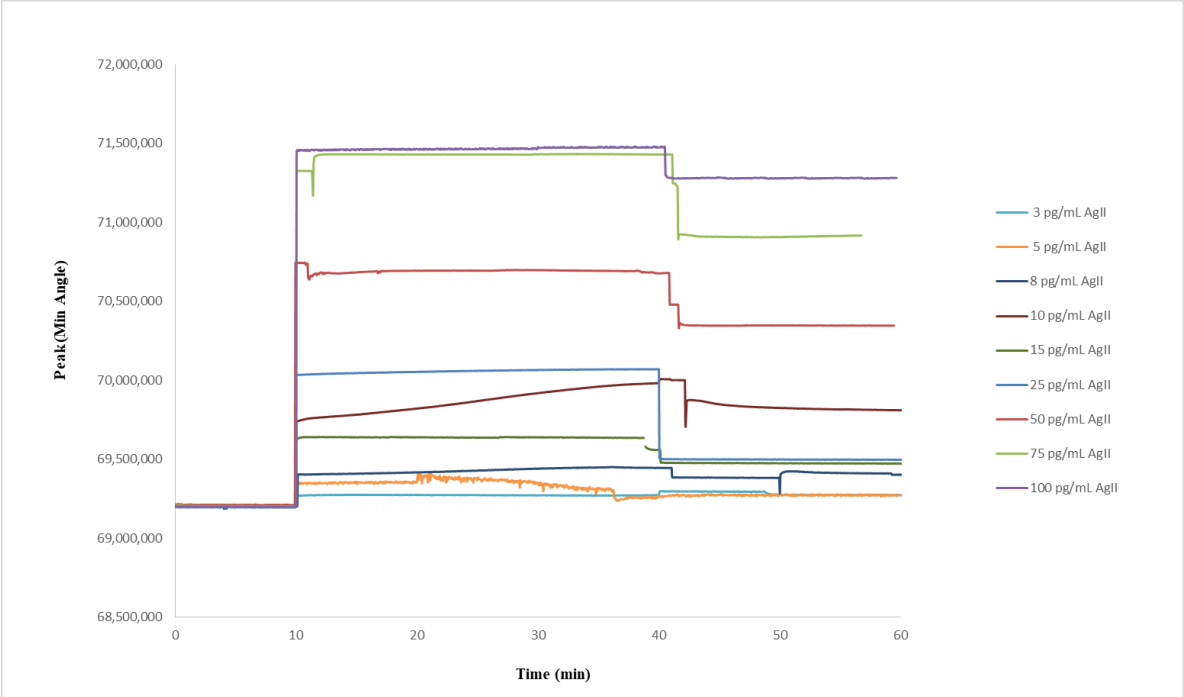

Figure 4.13. Sensorgrams of different AgII concentrations.

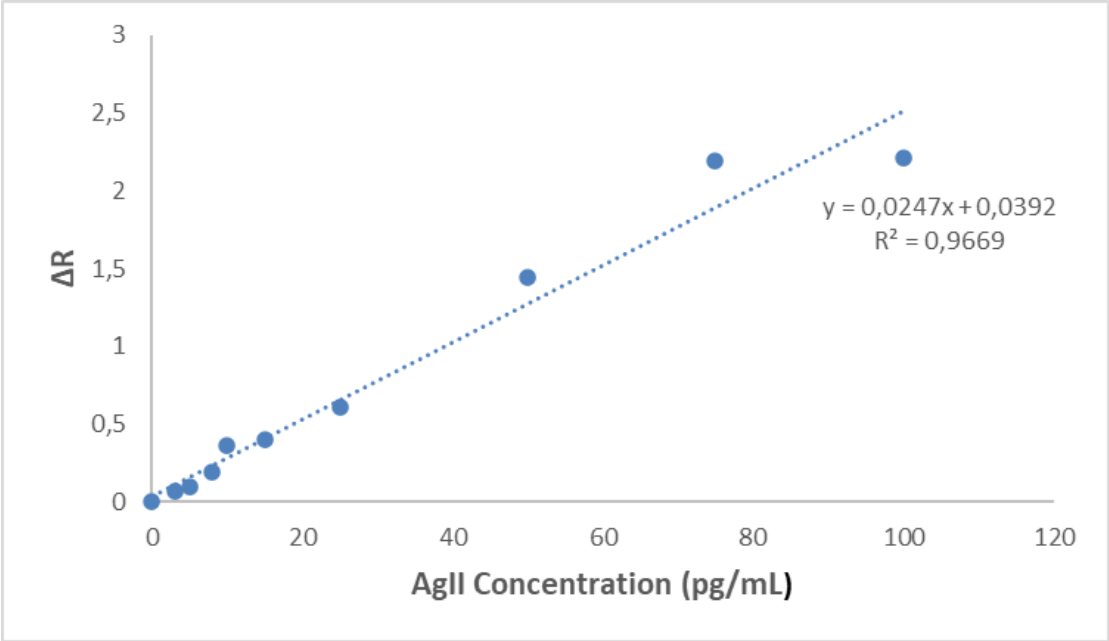

Figure 4.14. ΔR values acquired through the interaction of AgII solutions with AgII-MICspr chip.

4.5.1. Langmuir, Freundlich, and Langmuir-Freundlich Adsorption Isoterm Models

The isotherm models of AgII-MICspr sensor, constructed using AgII-MIP nanoparticles, were investigated. For this purpose, Langmuir, Freundlich, and Langmuir-Freundlich isotherm models were used. Three models are fundamental models used to describe adsorption processes.

According to Langmuir isotherm, adsorption takes place as a monolayer on a homogeneous surface, where adsorption ceases once a saturation point is reached (Tun and Chen, 2021). It can be mathematically represented as $\Delta R = (\Delta R_{max}[C])/(K_d+[C])$.
Freundlich isotherm is suitable for stratified adsorption across non-uniform surfaces due to its consideration of surface charge heterogeneity (Alsewailem, 2015) and expressed by $\Delta R = \Delta R_{max}[C]^{1/n}$.

Langmuir–Freundlich isotherm represents a combined approach, capturing the strengths of both classical isotherms. It is a hybrid model that accounts for monolayer adsorption on a homogeneous surface as well as multilayer adsorption due to surface heterogeneity (Alawode and Falode, 2019). This model is particularly useful when both monolayer and multilayer adsorption mechanisms are present in the system. The formula is $\Delta R = (\Delta R_{max}[C]^{1/n})/(K_d+[C]^{1/n})$. In the equations, ΔR_{max} corresponds to the maximum signal shift in SPR; C represents the AgII concentration; K_d is the dissociation equilibrium constant; and 1/n indicates the Freundlich surface heterogeneity index. The figures depicting the graphs generated by these three isotherm models are presented in **Figures 4.15 - 4.17.**

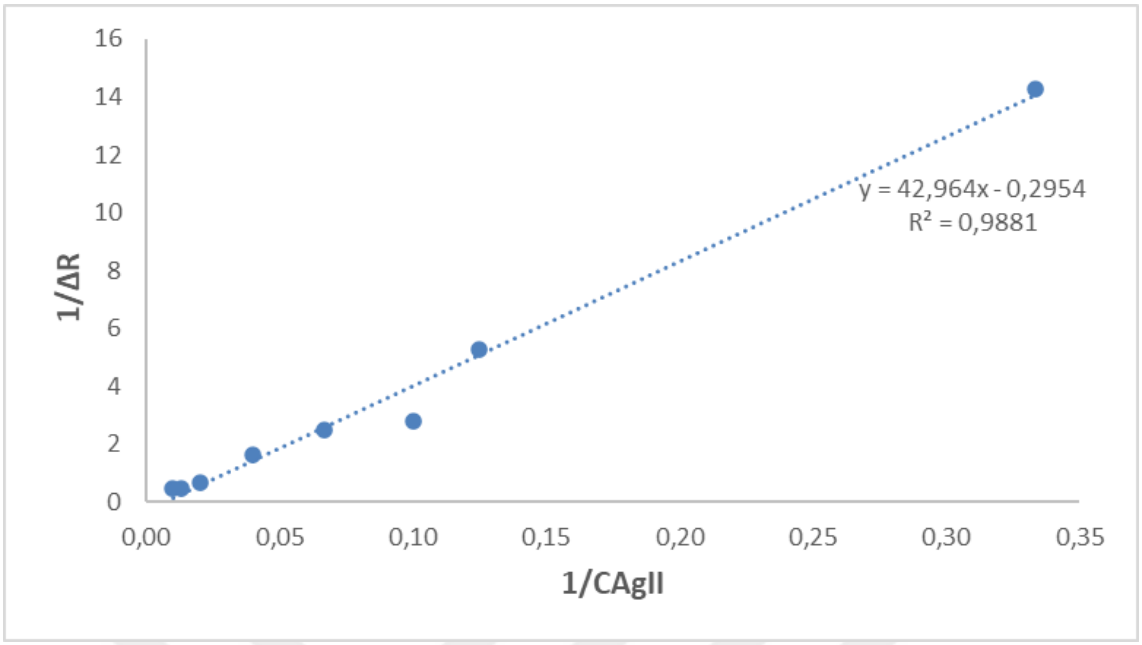

Figure 4.15. Langmuir model.

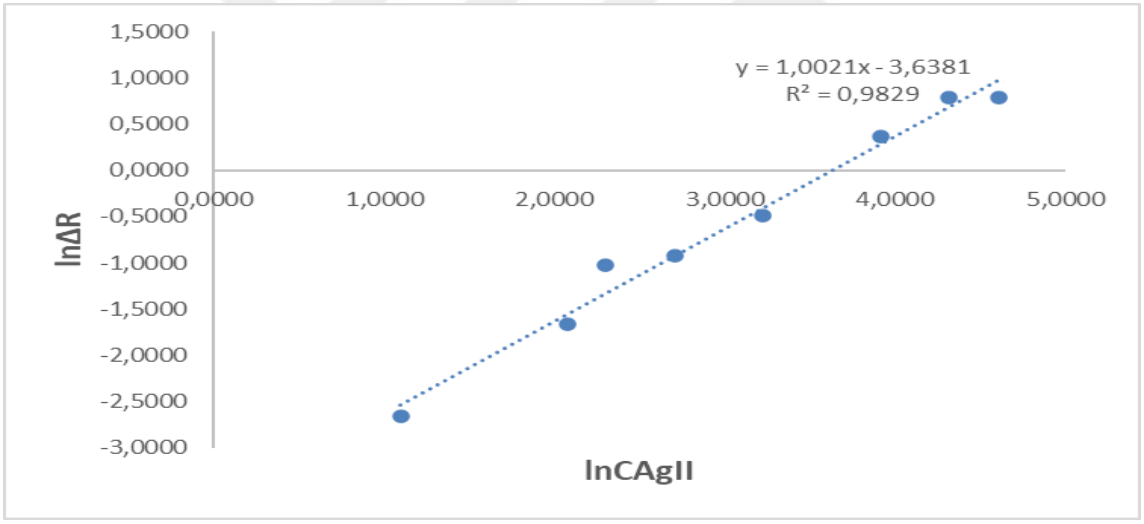

Figure 4.16. Freundlich model.

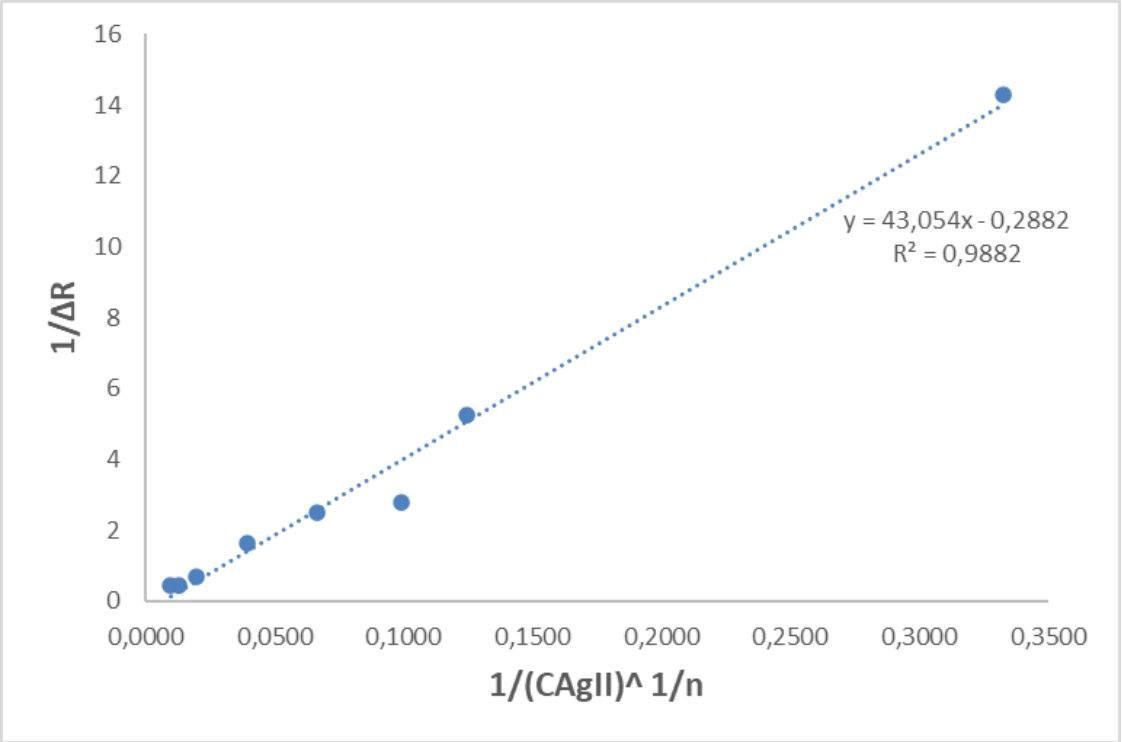

Figure 4.17. Langmuir- Freundlich model.

Table 4.1. Adsorption isotherm calculations.

	Langmuir	**Freundlich**	**Langmuir-Freundlich**
ΔR_{max}	3.3852	38.0195	3.4698
1/n	-	1.0021	1.0021
K_d	145.4435	-	149.3893
K_a	0.0069	-	0.0067
R^2	0.9881	0.9829	0.9882

The graphical data of the isotherm models (**Figures 4.15. - 4.17.**) along with their corresponding calculations (**Table 4.1**) are presented in detail, and the compatibility of the models with the experimental data is compared. As a result of these analyses, it was determined that the experimental data obtained are in high agreement with the Langmuir

isotherm model. This high agreement with the Langmuir model shows that the AgII-MIP nanoparticles form a monolayer bond on the chip surface and that the bonding regions are distributed homogeneously. This also reveals that there is no significant lateral interaction between the molecules during the bonding process.

4.6. AgII Competitive Binding Kinetic Analyzes using AgII-MICspr and NICspr Chips

The primary advantage of MIP-based SPR sensors is their capability to directly detect target molecules without the need for labels. The efficacy of the molecular imprinting process is closely linked to the selectivity of sensor. In the study, AgII-MICspr and NICspr chips were used to determine the selectivity of the nanoparticle-based SPR sensor. To control the selectivity, the competitor molecules AgI and Vp were used in addition to the target molecule AgII. Solutions of AgII, AgI, and Vp (15 pg/mL) were passed through the SPR sensor and the data indicated that the AgII-MICspr chip exhibited high selectivity for AgII in comparison to the NICspr chip. Additionally, it was determined that the selectivity of the AgII-MICspr chip towards AgII was 4.75 and 5.43 times higher than AgI and Vp molecules, respectively (**Figure 4.19., Table 4.2.**). Thereby, it was demonstrated that the prepared AgII-MICspr chip contained AgII-specific cavities, confirming the success of the imprinting process.

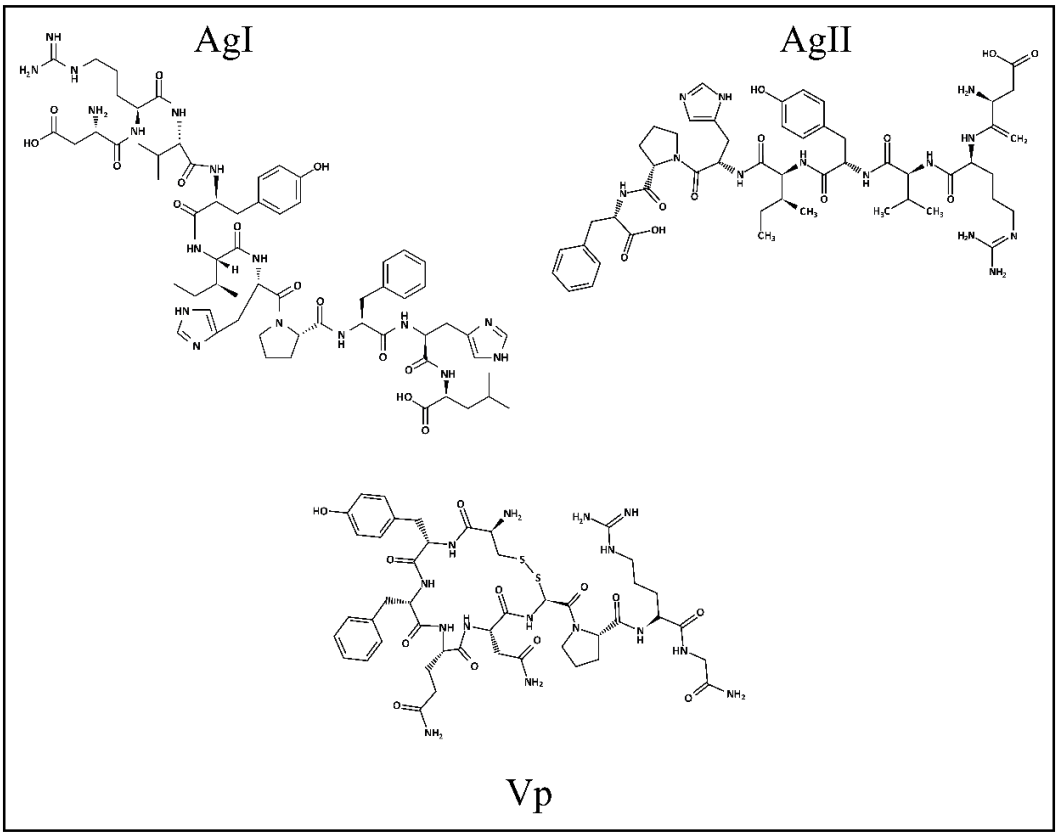

Figure 4.18. Chemical structures of AgI, AgII and Vp molecules.

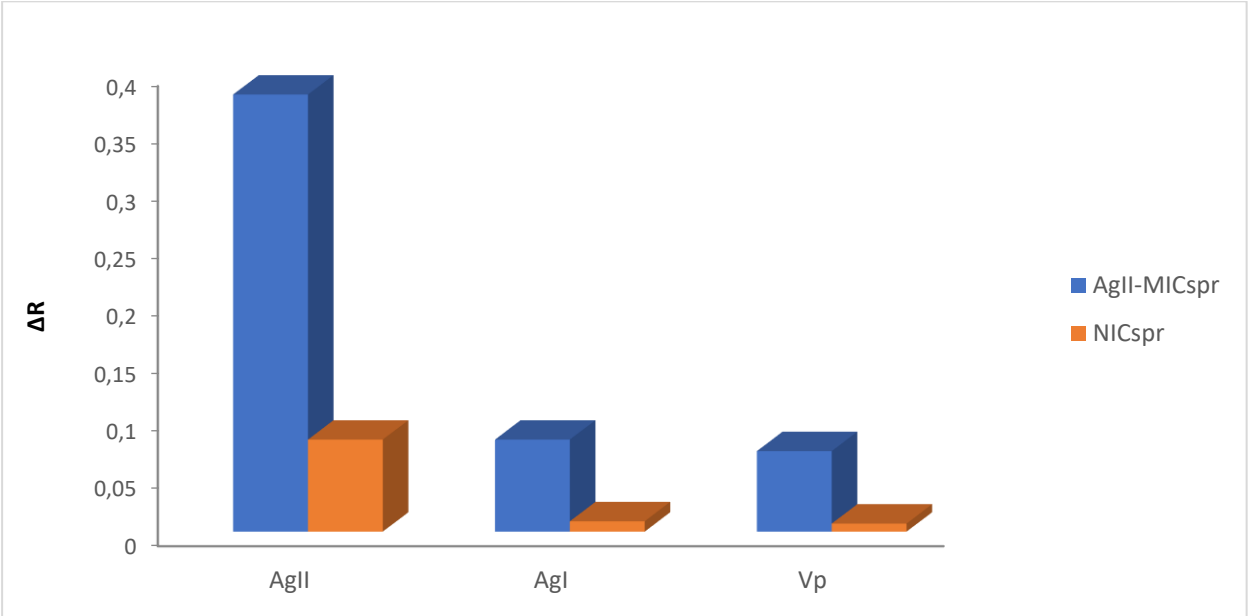

Figure 4.19. ΔR values of AgII, AgI and Vp molecules that passed through AgII-MICspr and NICspr-based SPR sensor systems.

Table 4.2. Selectivity and imprinting selectivity coefficients of AgII, AgI and Vp.

Molecules	ΔR_{MIP}	k_{MIP}	ΔR_{NIP}	k_{NIP}	k´
AgII	0.38	-	0.08	-	-
AgI	0.08	4.75	0.009	8.8889	0.534
Vp	0.07	5.43	0.007	11.4286	0.475

4.7. Reusability Studies

In order to investigate the repeated use of the AgII-MICspr chip, AgII prepared at 15 pg/mL concentrations was administered to the SPR device 10 consecutive times. Disassembly of AgII from the AgII-MICspr chip was done with NaCl (0.03 M) + PBS (10 mM, pH 7.4) solution. The results of 10 repeated experiments were presented in **Figure 4.20**. The continuous and stable response observed in the sensorgrams shows that the chip maintains its functionality in the binding regions and operates with the same sensitivity even with repeated use. These findings prove that the AgII-MICspr chip has been successfully designed and prepared, so it can be used repeatedly efficiently.

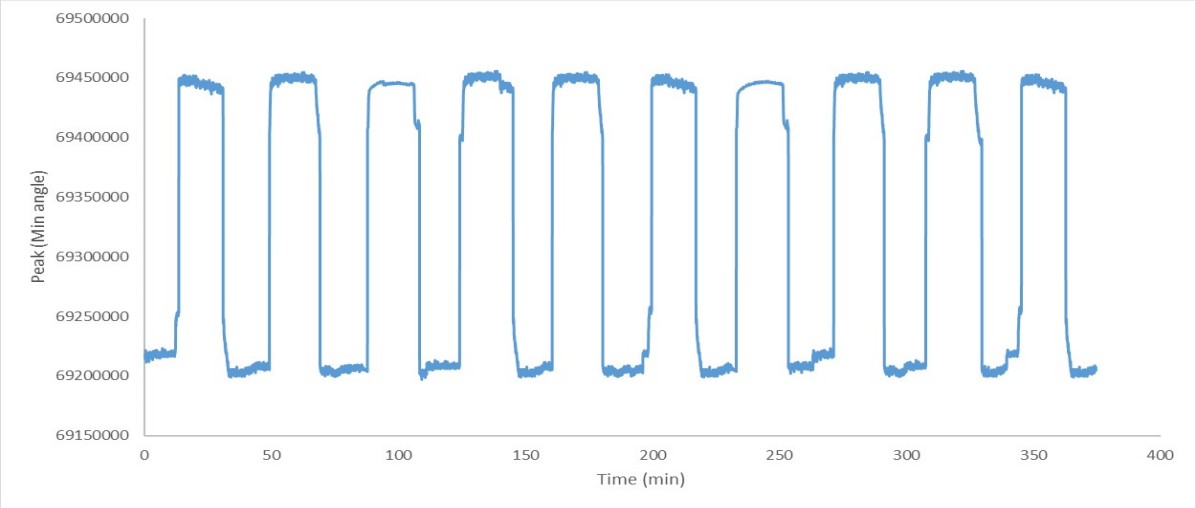

Figure 4.20. Reusability of AgII-MICspr chip.

4.8. AgII Detection from Human Serum Samples

The AgII-MICspr chip was exploited for the detection of AgII in human serum. The serum sample was diluted 1:10 and AgII was added to this diluted sample at different concentrations (3-100 pg/mL). As a result of the analyses, the sensorgrams obtained for each concentration are given in **Figure 4.21**. An increase in the peaks obtained was observed due to the increase in the concentration of AgII added to the serum sample. The findings indicated that AgII could be selectively detected at an exceptionally low concentration of 3 pg/mL from complex-containing samples like serum, utilizing the AgII-MICspr chip.

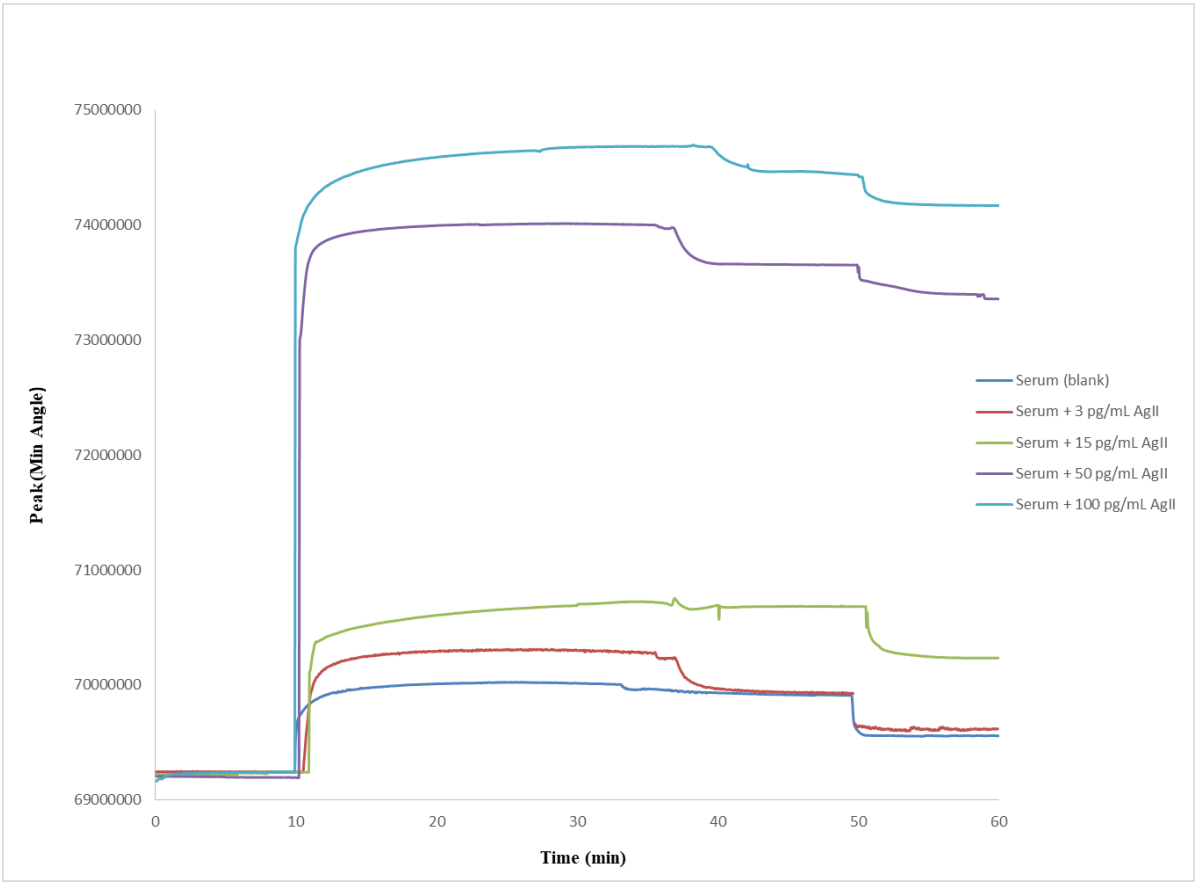

Figure 4.21. Sensorgrams of the AgII-MICspr chip with serum samples containing different concentrations of AgII.

5. CONCLUSION

Within the scope of the study, AgII-imprinted (AgII-MIP) and non-imprinted (NIP) (used as control) nanoparticles were prepared for the detection of AgII and their characterization (Zeta-size, TEM, SEM and FTIR) was performed. AgII-MIP and NIP nanoparticles measured 46.51 nm and 48.97 nm by Zetasizer, respectively. These nanoparticles were later applied to SPR chip surfaces to fabricate AgII-MIP and NIP nanoparticle-coated SPR chips (AgII-MICspr and NICspr). To verify the presence of AgII-MIP and NIP nanoparticles on the surfaces of AgII-MICspr and NICspr chips and to examine their surface characteristics and thickness, contact angle measurements and AFM analyses were carried out. Then, kinetic studies were conducted with AgII concentrations prepared in the concentration range of 3-100 pg/mL and it was observed that the AgII-MICspr chip could detect AgII at concentrations as low as 3 pg/mL. Competitor binding kinetic analysis studies were performed with AgI and Vp, which were selected as competitor molecules of AgII, and it was determined that the selectivity of the AgII-MICspr chip towards AgII was 4.75 and 5.43 times higher compared to these two competitor molecules, respectively. Reusability studies were performed and it was observed that the binding sites of the AgII-MICspr chip still maintained their functionality after 10 repetitions. Finally, by adding AgII to serum samples at concentrations of 3, 15, 50 and 100 pg/mL, the ability of the AgII-MICspr chip to selectively detect AgII in this complex environment containing different biomolecules was evaluated. Even in this environment, the chip was able to detect the lowest AgII concentration with high sensitivity. In light of the obtained data, it was shown that AgII can be detected rapidly, with high sensitivity and specificity with the developed AgII-MICspr chip. This study, based on the SPR sensor system coated with AgII-MIP nanoparticles, is of great importance in terms of filling the existing gap in the literature on AgII detection and pioneering in this field.

REFERENCES

Abdulhalim, I., Zourob, M., & Lakhtakia, A. (2008). Surface plasmon resonance for biosensing: a mini-review. Electromagnetics, 28(3), 214-242.

Akgönüllü, S., Kılıç, S., Esen, C., & Denizli, A. (2023). Molecularly imprinted polymer-based sensors for protein detection. Polymers, 15(3), 629.

Alawode, A. J., & Falode, O. A. (2019). Development of a new type-ı isotherm for correction of langmuir isotherm's over-estimation of adsorption at higher pressures. Physical Science International Journal, 23, 1-26.

Al-Bayati, M. & Al-Nahi, A. (2022). Determination of angiotensin-converting enzyme concentration in cardiovascular patients. International Journal of Health Sciences, 9661-9670.

Algieri, C., Drioli, E., Ahmed, C., Nasser, I., & Donato, L. (2014). Emerging tools for recognition and/or removal of dyes from polluted sites: molecularly imprinted membranes. Journal of Membrane and Separation Technology, 3(4), 243-266.

Alsewailem, F. D. (2015). Modified correlations for adsorption isotherms. Journal of Chemical & Engineering Data, 60(3), 762-765.

Ansari, M. T. I., Raghuwanshi, S. K., & Kumar, S. (2023). Recent Advancement in Fiber-Optic-Based SPR Biosensor for Food Adulteration Detection—A Review. IEEE Transactions on NanoBioscience, 22(4), 978-988.

Arabi, M., Ostovan, A., Li, J., Wang, X., Zhang, Z., Choo, J., & Chen, L. (2021). Molecular imprinting: green perspectives and strategies. Advanced Materials, 33(30), 2100543.

Asua, J. M. (2004). Emulsion polymerization: from fundamental mechanisms to process developments. Journal of Polymer Science Part A: Polymer Chemistry, 42(5), 1025-1041.

Bai, D., Lin, X., Huang, Y., & Zhang, X. (2018). Theranostics aspects of various nanoparticles in veterinary medicine. International Journal of Molecular Sciences, 19(11), 3299.

BelBruno, J. J. (2018). Molecularly imprinted polymers. Chemical Reviews, 119(1), 94-119.

Bellassai, N., D'Agata, R., Jungbluth, V., & Spoto, G. (2019). Surface plasmon resonance for biomarker detection: advances in non-invasive cancer diagnosis. Frontiers in Chemistry, 7, 570.

Bijhanmanesh, M. & Etesami, N. (2016). Continuous dosing of fast initiator during vinyl chloride suspension polymerization: polymerization rate and pvc properties. Journal of Applied Polymer Science, 133(41).

Binnig, G. & Rohrer, H. (1987). Scanning tunneling microscopy—from birth to adolescence. Reviews of Modern Physics, 59(3), 615-625.

Binnig, G., Quate, C. F., & Gerber, C. (1986). Atomic force microscope. Physical Review Letters, 56(9), 930-933.

Bleeker, E., Jong, W., Geertsma, R., Groenewold, M., Heugens, E., Koers-Jacquemijns, M., … & Oomen, A. (2013). Considerations on the eu definition of a nanomaterial: science to support policy making. Regulatory Toxicology and Pharmacology, 65(1), 119-125.

Busse, L. W., Wang, X. S., Chalikonda, D. M., Finkel, K. W., Khanna, A. K., Szerlip, H. M., ... & Chawla, L. S. (2017). Clinical experience with IV angiotensin II administration: a systematic review of safety. Critical Care Medicine, 45(8), 1285.

Butt, M. A. (2025). Surface plasmon resonance-based biodetection systems: Principles, progress and applications—A comprehensive review. Biosensors, 15(1), 35.

Camargo, R., Bombassaro, B., Monfort-Pires, M., Mansour, E., Palma, A., Ribeiro, L., … & Sposito, A. (2022). Plasma angiotensin ii is increased in critical coronavirus disease 2019. Frontiers in Cardiovascular Medicine, 9.

Capelli, D., Scognamiglio, V., & Montanari, R. (2023). Surface plasmon resonance technology: Recent advances, applications and experimental cases. TrAC Trends in Analytical Chemistry, 163, 117079.

Chen, L., Wang, X., Lü, W., Wu, X., & Li, J. (2016). Molecular imprinting: perspectives and applications. Chemical Society Reviews, 45(8), 2137-2211.

Chen, L., Xu, S., & Li, J. (2011). Recent advances in molecular imprinting technology: current status, challenges and highlighted applications. Chemical Society Reviews, 40(5), 2922.

Chen, T., Xin, J., Chang, S. J., Chen, C. J., & Liu, J. T. (2023). Surface plasmon resonance (SPR) combined technology: a powerful tool for investigating interface phenomena. Advanced Materials Interfaces, 10(8), 2202202.

Cheng, Z. J., Vapaatalo, H., & Mervaala, E. (2005). Angiotensin II and vascular inflammation. Medical Science Monitor, 11(6), 194-205.

Chhabra, K. H., Xia, H., Pedersen, K. B., Speth, R. C., & Lazartigues, E. (2013). Pancreatic angiotensin-converting enzyme 2 improves glycemia in angiotensin II-infused mice. American Journal of Physiology-Endocrinology and Metabolism, 304(8), E874-E884.

Cormack, P. A., & Elorza, A. Z. (2004). Molecularly imprinted polymers: synthesis and characterisation. Journal of Chromatography B, 804(1), 173-182.

Çaktü Güler, K., Göktürk, I., Yılmaz, F., Araz, A., & Denizli, A. (2024). Plasmonic nanosensors for environmental pollutants sensing: recent advances and perspectives. Essential Chem, 1(1), 1-19.

Damborský, P., Švitel, J., & Katrlík, J. (2016). Optical biosensors. Essays in Biochemistry, 60(1), 91-100.

Das, S., Devireddy, R., & Gartia, M. R. (2023). Surface plasmon resonance (SPR) sensor for cancer biomarker detection. Biosensors, 13(3), 396.

Ding, S., Lyu, Z., Niu, X., Zhou, Y., Liu, D., Falahati, M., ... & Lin, Y. (2020). Integrating ionic liquids with molecular imprinting technology for biorecognition and biosensing: a review. Biosensors and Bioelectronics, 149, 111830.

Duraisamy, S., Faulkner, J., Choudhury, G., Abboud, H., & Kasinath, B. (2001). Angiotensin ii inhibits insulin-stimulated phosphorylation of eukaryotic initiation factor 4e-binding protein-1 in proximal tubular epithelial cells. Biochemical Journal, 360(1), 87.

Ealia, S. A. M., & Saravanakumar, M. P. (2017, November). A review on the classification, characterisation, synthesis of nanoparticles and their application. In IOP conference series: materials science and engineering (Vol. 263, No. 3, p. 032019). IOP Publishing.

Elhachem, M., Bou-Maroun, E., Abboud, M., Cayot, P., & Maroun, R. G. (2023). Optimization of a molecularly imprinted polymer synthesis for a rapid detection of caffeic acid in wine. Foods, 12(8), 1660.

Englebienne, P., Van Hoonacker, A., & Verhas, M. (2003). Surface plasmon resonance: principles, methods and applications in biomedical sciences. Spectroscopy, 17(2-3), 255-273.

Erdem, Ö., Saylan, Y., Cihangir, N., & Denizli, A. (2019). Molecularly imprinted nanoparticles based plasmonic sensors for real-time Enterococcus faecalis detection. Biosensors and Bioelectronics, 126, 608-614.

Ertürk, G. & Mattìasson, B. (2017). Molecular imprinting techniques used for the preparation of biosensors. Sensors, 17(2), 288.

Ertürk, G., Özen, H., Tümer, M. A., Mattiasson, B., Denizli, A. (2016). Microcontact imprinting based surface plasmon resonance (SPR) biosensor for real-time and ultrasensitive detection of prostate specific antigen (PSA) from clinical samples, Sensors and Actuators B: Chemical, 224, 823-832.

Esentürk, M. K., Akgönüllü, S., Yılmaz, F., & Denizli, A. (2019). Molecularly imprinted based surface plasmon resonance nanosensors for microalbumin detection. Journal of Biomaterials Science, Polymer Edition, 30(8), 646-661.

Fuloria, S., Subramaniyan, V., Meenakshi, D. U., Sekar, M., Chakravarthi, S., Kumar, D. H., ... & Fuloria, N. K. (2022). Etiopathophysiological role of the renin–angiotensin–aldosterone system in age-related muscular weakening: RAAS-independent beneficial role of ACE2 in muscle weakness. Journal of Biochemical and Molecular Toxicology, 36(6), e23030.

Gard, P. R. (2002). The role of angiotensin II in cognition and behaviour. European Journal of Pharmacology, 438(1-2), 1-14.

Garip, M., Arslan, E., Prabowo, S., & Keskin, H. (2022). Investigating the uses of ‘’nanotechnology’’ as an alternative approach to increasing animal welfare in dairy cattle. Erciyes Üniversitesi Veteriner Fakültesi Dergisi, 19(1), 67-73.

Gitea, D., Teodorescu, A. G., Pantiş, C., Ţiţ, D. M., Bungău, A. F., Bogdan, M. A., … & Bustea, C. (2020). Green synthesis of silver nanoparticles using hypericum perforatum l. extract and evaluation of their antibacterial activity. Revista De Chimie, 71(2), 273-279.

Gong, S., Yu, Z., Meng, L., Hu, L., & He, Y. (2004). Dye-molecular-imprinted polysiloxanes. ii. preparation, characterization, and recognition behavior. Journal of Applied Polymer Science, 93(2), 637-643.

Gour, A. & Jain, N. (2019). Advances in green synthesis of nanoparticles. Artificial Cells Nanomedicine and Biotechnology, 47(1), 844-851.

Guan, X., Zhou, Y., & Li, J. (2011). Reciprocal roles of angiotensin ii and angiotensin ii receptors blockade (arb) in regulating cbfa1/rankl via camp signaling pathway: possible mechanism for hypertension-related osteoporosis and antagonistic effect of arb on hypertension-related osteoporosis. International Journal of Molecular Sciences, 12(7), 4206-4213.

Gundogdu, A., Gazoglu, G., Kahraman, E., Yildiz, E., Candir, G., Yalcin, D., ... & Şen, F. (2023). Biosensors: Types, applications, and future advantages. Journal of Scientific Reports-A, (052), 457-481.

Hasanah, A. N., Safitri, N., Zulfa, A., Neli, N., & Rahayu, D. (2021). Factors affecting preparation of molecularly imprinted polymer and methods on finding template-monomer interaction as the key of selective properties of the materials. Molecules, 26(18), 5612.

Hayden, M. R., Habibi, J., Joginpally, T., Karuparthi, P. R., & Sowers, J. R. (2012). Ultrastructure study of transgenic Ren2 rat aorta–part 1: endothelium and intima. Cardiorenal Medicine, 2(1), 66-82.

Herrera-Domínguez, M., Morales-Luna, G., Mahlknecht, J., Cheng, Q., Aguilar-Hernández, I., & Ornelas-Soto, N. (2023). Optical biosensors and their applications for the detection of water pollutants. Biosensors, 13(3), 370.

Homola, J. (2008). Surface plasmon resonance sensors for detection of chemical and biological species. Chemical Reviews, 108(2), 462-493.

Homola, J. (2009, June). Surface plasmon resonance biosensing. In The European Conference on Lasers and Electro-Optics (p. CH5_3). Optica Publishing Group.

Hulla, J. E., Sahu, S. C., & Hayes, A. W. (2015). Nanotechnology: history and future. Human & Experimental Toxicology, 34(12), 1318-1321.

Kalecki, J., Cieplak, M., Iskierko, Z., Piechowska, J., Nogala, W., D'Souza, F., … & Sharma, P. S. (2023). Post-imprinting modification: electrochemical and scanning electrochemical microscopy studies of a semi-covalently surface imprinted polymer. Journal of Materials Chemistry B, 11(8), 1659-1669.

Kamal Eddin, F. B., & Fen, Y. W. (2020). The principle of nanomaterials based surface plasmon resonance biosensors and its potential for dopamine detection. Molecules, 25(12), 2769.

Karunakaran, C., Rajkumar, R., & Bhargava, K. (2015). Introduction to Biosensors. Biosensors and Bioelectronics, 1–68.

Katas, H., Moden, N. Z., Lim, C. S., Celesistinus, T., Chan, J. Y., Ganasan, P., … & Abdalla, S. S. I. (2018). Biosynthesis and potential applications of silver and gold nanoparticles and their chitosan-based nanocomposites in nanomedicine. Journal of Nanotechnology, 2018, 1-13.

Klębowski, B., Depciuch, J., Parlińska-Wojtan, M., & Baran, J. (2018). Applications of noble metal-based nanoparticles in medicine. International Journal of Molecular Sciences, 19(12), 4031.

Kotoulas, C., & Kiparissides, C. (2006). A generalized population balance model for the prediction of particle size distribution in suspension polymerization reactors. Chemical Engineering Science, 61(2), 332-346.

Kurra, N. & Reifenberger, R. (2014). Nanocarbon-scanning probe microscopy synergy: fundamental aspects to nanoscale devices. Acs Applied Materials & Interfaces, 6(9), 6147-6163.

Lacher, N., Garrison, K., & Lunte, S. (2002). Separation and detection of angiotensin peptides by cu(ii) complexation and capillary electrophoresis with uv and electrochemical detection. Electrophoresis, 23(11), 1577.

Lamb, R. E., & Folstad, J. (2003). Aldosterone receptor antagonists: focus on eplerenone. Progress in Cardiovascular Nursing, 18(1), 54-59.

Lawal, S. K., Olojede, S. O., Faborode, O. S., Aladeyelu, O. S., Matshipi, M. N., Sulaiman, S. O., … & Azu, O. O. (2022). Nanodelivery of antiretroviral drugs to nervous tissues. Frontiers in Pharmacology, 13.

Leisman, D., Privratsky, J., Lehman, J., Abraham, M., Yaipan, O., Brewer, M., … & Taylor, M. (2022). Angiotensin ii enhances bacterial clearance via myeloid signaling in a murine sepsis model. Proceedings of the National Academy of Sciences, 119(34).

Li, R., Feng, Y., Pan, G., & Liu, L. (2019). Advances in molecularly imprinting technology for bioanalytical applications. Sensors, 19(1), 177.

Li, W., Chen, M., Xiong, H., Wen, W., He, H., & Zhang, X. (2016). Surface protein imprinted magnetic nanoparticles for specific recognition of bovine hemoglobin. New Journal of Chemistry, 40(1), 564-570.

Lillyblad, M. P., Knutson, A. R., Philbrick, A. M., & Westberg, S. M. (2012). Aliskiren alone or in combination for the treatment of mild-to-moderate hypertension: current role and future perspectives. Journal of Pharmacy Technology, 28(1), 16-25.

Lindpaintner, K., Jin, M. W., Niedermaier, N., Wilhelm, M. J., & Ganten, D. (1990). Cardiac angiotensinogen and its local activation in the isolated perfused beating heart. Circulation Research, 67(3), 564-573.

Liu, G., Huang, X., Li, L., Xu, X., Zhang, Y., Lv, J., … & Xu, D. (2019). Recent advances and perspectives of molecularly imprinted polymer-based fluorescent sensors in food and environment analysis. Nanomaterials, 9(7), 1030.

Liu, Q., Wu, C., Hua, C., Hu, N., Zhou, J., & Wang, P. (2014). Cell-based biosensors and their application in biomedicine. Chemical Reviews, 114(12), 6423-6461.

Liu, Y., Yang, Y., Zhang, C., Huang, F., Wang, F., Yuan, J., ... & Liu, L. (2020). Clinical and biochemical indexes from 2019-nCoV infected patients linked to viral loads and lung injury. Science China Life Sciences, 63, 364-374.

Ma, W., Tang, B., & Row, K. H. (2017). Exploration of a ternary deep eutectic solvent of methyltriphenylphosphonium bromide/chalcone/formic acid for the selective recognition of rutin and quercetin in herba artemisiae scopariae. Journal of Separation Science, 40(16), 3248-3256.

Manickam, P., Arizaleta, F., Muneeswaran, G., & Bhansali, S. (2017). Theoretical studies of cortisol-imprinted prepolymerization mixtures: structural insights into improving the selectivity of affinity sensors. Journal of the Electrochemical Society, 164(5), B3077-B3080.

Mascolo, A., Scavone, C., Rafaniello, C., De Angelis, A., Urbanek, K., di Mauro, G., ... & Capuano, A. (2021). The role of renin-angiotensin-aldosterone system in the heart and lung: focus on COVID-19. Frontiers in Pharmacology, 12, 667254.

McDonnell, J. M. (2001). Surface plasmon resonance: towards an understanding of the mechanisms of biological molecular recognition. Current Opinion in Chemical Biology, 5(5), 572-577.

Mehrotra, P. (2016). Biosensors and their applications–A review. Journal of Oral Biology and Craniofacial Research, 6(2), 153-159.

Mehrvar, M., & Abdi, M. (2004). Recent developments, characteristics, and potential applications of electrochemical biosensors. Analytical Sciences, 20(8), 1113-1126.

Meng, J., Gao, X., Zhang, J., He, X., Ou, M., Bi, J., … & Zhang, G. (2020). Renin-angiotensin system inhibitors improve the clinical outcomes of covid-19 patients with hypertension. Emerging Microbes & Infections, 9(1), 757-760.

Meretskyi, V., Meretska, I., Kulyanda, O., & Kamtoh, G. (2017). Direct renin inhibitors in arterial hypertension treatment. Scientific Journal of Polonia University, 25(6), 146-154.

Mohamed, E. (2017). Nanotechnology: future of environmental air pollution control. Environmental Management and Sustainable Development, 6(2), 429.

Morishita, Y., & Kusano, E. (2013). Direct Renin inhibitor: aliskiren in chronic kidney disease. Nephro-urology Monthly, 5(1), 668.

Mostafa, A. M., Barton, S. J., Wren, S. P., & Barker, J. (2021). Review on molecularly imprinted polymers with a focus on their application to the analysis of protein biomarkers. TrAC Trends in Analytical Chemistry, 144, 116431.

Motamedi, M., Yerushalmi, L., Haghighat, F., & Chen, Z. (2022). Recent developments in photocatalysis of industrial effluents: A review and example of phenolic compounds degradation. Chemosphere, 296, 133688.

Ni, W., Yang, X., Yang, D., Bao, J., Li, R., Xiao, Y., ... & Gao, Z. (2020). Role of angiotensin-converting enzyme 2 (ACE2) in COVID-19. Critical Care, 24, 1-10.

Olson, S., Oeckler, R., Li, X., Du, L., Traganos, F., Zhao, X., … & Burke-Wolin, T. (2004). Angiotensin ii stimulates nitric oxide production in pulmonary artery endothelium via the type 2 receptor. Ajp Lung Cellular and Molecular Physiology, 287(3), L559-L568.

Ondráček, M., Pou, P. J., Rozsíval, V., González, C., Jelínek, P., & Pérez, R. (2011). Forces and currents in carbon nanostructures: are we imaging atoms?. Physical Review Letters, 106(17).

Park, J. H., Cho, Y. W., & Kim, T. H. (2022). Recent advances in surface plasmon resonance sensors for sensitive optical detection of pathogens. Biosensors, 12(3), 180.

Patel, S., Rauf, A., Khan, H., & Abu-Izneid, T. (2017). Renin-angiotensin-aldosterone (RAAS): The ubiquitous system for homeostasis and pathologies. Biomedicine & Pharmacotherapy, 94, 317-325.

Perumal, V., & Hashim, U. (2014). Advances in biosensors: Principle, architecture and applications. Journal of Applied Biomedicine, 12(1), 1-15.

Popp, R., Li, Y., LeBlanc, A., Mohammed, Y., Aguilar-Mahecha, A., Chambers, A., … & Borchers, C. (2017). Immuno-matrix-assisted laser desorption/ionization assays for quantifying akt1 and akt2 in breast and colorectal cancer cell lines and tumors. Analytical Chemistry, 89(19), 10592-10600.

Poulsen, S. B., & Fenton, R. A. (2019). K+ and the renin–angiotensin–aldosterone system: New insights into their role in blood pressure control and hypertension treatment. The Journal of Physiology, 597(17), 4451-4464.

Qi, P., Wang, J., Wang, L., Li, Y., Jin, J., Su, F., … Chen, J. (2010). Molecularly imprinted polymers synthesized via semi-covalent imprinting with sacrificial spacer for imprinting phenols. Polymer, 51(23), 5417–5423.

Raj, A., Shetty, N. J., & Ali, A. (2023). Role of nanotechnology in dentistry: a systematic review. Journal of Stomatology, 76(2), 136-140.

Ramanavièius, A., Herberg, F. W., Hutschenreiter, S., Zimmermann, B., Lapënaitë, I., Kaušaitë, A., ... & Ramanavièienë, A. (2005). Biomedical application of surface plasmon resonance biosensors. Acta Medica Lituanica, 12(3).

Ravindran, N., Kumar, S., Yashini, M., Rajeshwari, S., Mamathi, C. A., Thirunavookarasu, S, N., & Sunil, C. K. (2023). Recent advances in surface plasmon resonance (SPR) biosensors for food analysis: A review. Critical Reviews in Food Science and Nutrition, 63(8), 1055-1077.

Rich, R. L., & Myszka, D. G. (2000). Advances in surface plasmon resonance biosensor analysis. Current Opinion in Biotechnology, 11(1), 54-61.

Rocheleau, G., Lee, T., Mohammed, Y., Burns, K., Cheng, M., Tran, K., … & Russell, J. (2022). Renin-angiotensin system pathway therapeutics associated with improved outcomes in males hospitalized with covid-19*. Critical Care Medicine, 50(9), 1306-1317.

Sajini, T., & Mathew, B. (2021). A brief overview of molecularly imprinted polymers: Highlighting computational design, nano and photo-responsive imprinting. Talanta Open, 4, 100072.

Saleem, H. & Zaidi, S. (2020). Sustainable use of nanomaterials in textiles and their environmental impact. Materials, 13(22), 5134.

Saleem, H. & Zaidi, S. J. (2020). Recent developments in the application of nanomaterials in agroecosystems. Nanomaterials, 10(12), 2411.

Saylan, Y., Erdem, Ö., Ünal, S., & Denizli, A. (2019). An alternative medical diagnosis method: biosensors for virus detection. Biosensors, 9(2), 65.

Saylan, Y., Yılmaz, F., Özgür, E., Derazshamshir, A., Yavuz, H., & Denizli, A. (2017). Molecular imprinting of macromolecules for sensor applications. Sensors, 17(4), 898.

Schaming, D., & Remita, H. (2015). Nanotechnology: from the ancient time to nowadays. Foundations of Chemistry, 17, 187-205.

Schulz, A., Jankowski, J., Zidek, W., & Jankowski, V. (2014). Absolute quantification of endogenous angiotensin ii levels in human plasma using esi-lc-ms/ms. Clinical Proteomics, 11(1).

Shafiq, M., Anjum, S., Hano, C., Anjum, I., & Abbasi, B. H. (2020). An overview of the applications of nanomaterials and nanodevices in the food industry. Foods, 9(2), 148.

Sharma, C., Dhiman, R., Rokana, N., & Panwar, H. (2017). Nanotechnology: an untapped resource for food packaging. Frontiers in Microbiology, 8.

Shi, Z., Chow, C., Fabris, R., Liu, J., & Jin, B. (2022). Applications of online uv-vis spectrophotometer for drinking water quality monitoring and process control: a review. Sensors, 22(8), 2987.

Shin, W. K., Cho, J., Kannan, A. G., Lee, Y. S., & Kim, D. W. (2016). Cross-linked composite gel polymer electrolyte using mesoporous methacrylate-functionalized SiO2 nanoparticles for lithium-ion polymer batteries. Scientific Reports, 6(1), 26332.

Sriramula, S., Haque, M., Majid, D. S., & Francis, J. (2008). Involvement of tumor necrosis factor-α in angiotensin II–mediated effects on salt appetite, hypertension, and cardiac hypertrophy. Hypertension, 51(5), 1345-1351.

Sun, M. & Gupta, A. (2019). Vascular nanomedicine: current status, opportunities, and challenges. Seminars in Thrombosis and Hemostasis, 46(05), 524-544.

Şerbetçi, T., & Boğa, B. (2022). Renin-anjiyotensin-aldosteron sistemine etkili tıbbi bitkilerin potansiyel kullanımı. KTO Karatay Üniversitesi Sağlık Bilimleri Dergisi, 3(1), 105-118.

Takeuchi, T. & Matsui, J. (1996). Molecular imprinting: an approach to "tailor-made" synthetic polymers with biomimetic functions. Acta Polymerica, 47(11-12), 471-480.

Tan, A., Chawla, R., Natasha, G., Mahdibeiraghdar, S., Jeyaraj, R., Rajadas, J., … & Seifalian, A. (2016). Nanotechnology and regenerative therapeutics in plastic surgery: the next frontier. Journal of Plastic Reconstructive & Aesthetic Surgery, 69(1), 1-13.

Tang, Y., Lan, J., Gao, X., Liu, X., Zhang, D., Wei, L., … & Li, J. (2016). Determination of clenbuterol in pork and potable water samples by molecularly imprinted polymer through the use of covalent imprinting method. Food Chemistry, 190, 952-959.

Tun, H., & Chen, C. C. (2021). Isosteric heat of adsorption from thermodynamic langmuir isotherm. Adsorption, 27(6), 979-989.

Vahabi, S., Salman, B. N., & Javanmard, A. (2013). Atomic force microscopy application in biological research: a review study. Iranian Journal of Medical Sciences, 38(2), 76.

Van Dorst, B., Mehta, J., Bekaert, K., Rouah-Martin, E., De Coen, W., Dubruel, P., ... & Robbens, J. (2010). Recent advances in recognition elements of food and environmental biosensors: A review. Biosensors and Bioelectronics, 26(4), 1178-1194.

Vasapollo, G., Sole, R., Mergola, L., Lazzoi, M., Scardino, A., Scorrano, S., … & Mele, G. (2011). Molecularly imprinted polymers: present and future prospective. International Journal of Molecular Sciences, 12(9), 5908-5945.

Verma, S., Chevvuri, R., & Sharma, H. (2018). Nanotechnology in dentistry: unleashing the hidden gems. Journal of Indian Society of Periodontology, 22(3), 196.

Vigneshvar, S., Sudhakumari, C. C., Senthilkumaran, B., & Prakash, H. (2016). Recent advances in biosensor technology for potential applications–an overview. Frontiers in Bioengineering and Biotechnology, 4, 11.

Virkutytė, J. & Varma, R. (2011). Green synthesis of metal nanoparticles: biodegradable polymers and enzymes in stabilization and surface functionalization. Chemical Science, 2(5), 837-846.

Vivaldo-Lima, E., Wood, P. E., Hamielec, A. E., & Penlidis, A. (1997). An updated review on suspension polymerization. Industrial & Engineering Chemistry Research, 36(4), 939–965.

Volpe, M., Danser, A. J., Menard, J., Waeber, B., Mueller, D. N., Maggioni, A. P., & Ruilope, L. M. (2012). Inhibition of the renin–angiotensin–aldosterone system: is there room for dual blockade in the cardiorenal continuum?. Journal of Hypertension, 30(4), 647-654.

Wang, L., Lin, F., & Yu, L. (2012). A molecularly imprinted photonic polymer sensor with high selectivity for tetracyclines analysis in food. The Analyst, 137(15), 3502.

Wang, L., Teles, M. P., Arabkoohsar, A., Yu, H., Ismail, K. A. R., & Mahian, O. (2022). A holistic and state-of-the-art review of nanotechnology in solar cells. Sustainable Energy Technologies and Assessments, 54, 102864.

Webster, T. J., Tong, Z., Liu, J., & Banks, M. K. (2005). Adhesion ofpseudomonas fluorescensonto nanophase materials. Nanotechnology, 16(7), S449-S457.

Webster, T., Liu, J., & Banks, M. (2004). More efficient capture of bacteria on nanostructured materials. Mrs Proceedings, 845.

Willander, M., & Al-Hilli, S. (2009). Analysis of biomolecules using surface plasmons. Micro and Nano Technologies in Bioanalysis: Methods and Protocols, 201-229.

Włoch, M., & Datta, J. (2019). Synthesis and polymerisation techniques of molecularly imprinted polymers. In Comprehensive analytical chemistry (Vol. 86, pp. 17-40). Elsevier.

Wohlleben, W., Mielke, J., Bianchin, A., Ghanem, A., Freiberger, H., Rauscher, H., … & Hodoroabă, V. (2017). Reliable nanomaterial classification of powders using the volume-specific surface area method. Journal of Nanoparticle Research, 19(2).

Yan, H., & Row, K. H. (2006). Characteristic and synthetic approach of molecularly imprinted polymer. International Journal of Molecular Sciences, 7(5), 155-178.

Yıldırım, M., & Baydemir Peşint, G. (2021). Molecularly imprinted spongy columns for angiotensin (ii) recognition from human serum. Biotechnology Progress, 37(2), e3112.

Yu, H., Regulacio, M. D., Ye, E., & Han, M. (2013). Chemical routes to top-down nanofabrication. Chemical Society Reviews, 42(14), 6006.

Yuan, H., Khoury, C., Hwang, H., Wilson, C., Grant, G., & Vo-Dinh, T. (2012). Gold nanostars: surfactant-free synthesis, 3d modelling, and two-photon photoluminescence imaging. Nanotechnology, 23(7), 075102.

Zhang, F., Luo, M., Chen, Z., Wei, Z., & Pinnavaia, T. (2013). Effects of mesoporous silica particles on the emulsion polymerization of methyl methacrylate. Polymer Engineering & Science, 54(12), 2746-2752.

Zhang, H., Penninger, J. M., Li, Y., Zhong, N., & Slutsky, A. S. (2020). Angiotensin-converting enzyme 2 (ACE2) as a SARS-CoV-2 receptor: molecular mechanisms and potential therapeutic target. Intensive Care Medicine, 46, 586-590.

Zhang, H., Ye, L., & Mosbach, K. (2006). Non-covalent molecular imprinting with emphasis on its application in separation and drug development. Journal of Molecular Recognition, 19(4), 248–259.

Zhang, J., Hui, Y., Liu, F., Yang, Q., Lu, Y., Chang, Y., … & Ding, Y. (2022). Neohesperidin protects angiotensin ii-induced hypertension and vascular remodeling. Frontiers in Pharmacology, 13.

Zhang, S., Jia, Z., Liu, T., Wei, G., & Su, Z. (2019). Electrospinning nanoparticles-based materials interfaces for sensor applications. Sensors, 19(18), 3977.

Zhang, Y., Tang, H., Chen, W., & Zhang, J. (2022). Nanomaterials used in fluorescence polarization based biosensors. International Journal of Molecular Sciences, 23(15), 8625.

Zhang, Y., Yuan, X., Jiang, W., & Liu, H. (2020). Determination of nereistoxin-related insecticide via quantum-dots-doped covalent organic frameworks in a molecularly imprinted network. Microchimica Acta, 187, 1-9.

Zhu, Y., Pan, Z., Rong, J., Mao, K., Yang, D., Zhang, T., ... & Pan, J. (2021). Boronate affinity surface imprinted polymers supported on dendritic fibrous silica for enhanced selective separation of shikimic acid via covalent binding. Journal of Molecular Liquids, 337, 116408.

Zietek, M., Fita, K., Diakowska, D., Watras, A., & Wiglusz, R. J. (2021). In vitro studies concerning selected properties of a composite material blended with nanofluoroapatite crystals. Materials, 14(23), 7295.

Zink, S., Moura, F., Autreto, P., Galvao, D., & Mizaikoff, B. (2018). Virtually imprinted polymers (vips): understanding molecularly templated materialsviamolecular dynamics simulations. Physical Chemistry Chemical Physics, 20(19), 13145-13152.